Journal of Medicinal Chemistry

Article

Function-oriented development of CXCR4 antagonists as selective Human Immunodeficiency Virus (HIV)-1 entry inhibitors

Chien-Huang Wu, Chuan- Jen Wang, Chun-Ping Chang, Yung-Chi Cheng, Jen-Shin Song, Jiing-Jyh Jan, Ming-Chen Chou, Yi-Yu Ke, Jing Ma, Ying-Chieh Wong, Tsung-Chih Hsieh, Yun-Chen Tien, Elizabeth A. Gullen, Chen-Fu Lo, Chia-Yi Cheng, Yu-Wei Liu, Amit A. Sadani, Chia-Hua Tsai, Hsing-Pang Hsieh, Lun Kelvin Tsou, and Kak-Shan Shia

J. Med. Chem., **Just Accepted Manuscript** • DOI: 10.1021/jm501772w • Publication Date (Web): 13 Jan 2015

	Tsou, Lun; National Health Research Institutes, Institute of Biotechnology and Pharmaceutical Research Shia, Kak-Shan; National Health Research Institutes, Institute of Biotechnology and Pharmaceutical Research

Function-oriented development of CXCR4 antagonists as selective Human Immunodeficiency Virus (HIV)-1 entry inhibitors

Chien-Huang Wu,[†a] Chuan-Jen Wang,[†b] Chun-Ping Chang,[a] Yung-Chi Cheng,[b] Jen-Shin Song,[a] Jiing-Jyh Jan,[a] Ming-Chen Chou,[a] Yi-Yu Ke,[a] Jing Ma,[c] Ying-Chieh Wong,[a] Tsung-Chih Hsieh,[a] Yun-Chen Tien,[b] Elizabeth A. Gullen,[b] Chen-Fu Lo,[a] Chia-Yi Cheng,[a] Yu-Wei Liu,[a] Amit A. Sadani,[a] Chia-Hua Tsai,[a] Hsin-Pang Hsieh,[a] Lun K. Tsou,*[a] and Kak-Shan Shia*[a]

[a] Institute of Biotechnology and Pharmaceutical Research, National Health Research Institutes, Miaoli County 35053, Taiwan, R.O.C.

[b] Department of Pharmacology, Yale University School of Medicine, New Haven, CT 06520, USA.

[c] Liver Diseases Center, Department of Infectious Diseases, Second Xiangya Hospital, Central South University, Hunan Province, China.

ABSTRACT

Motivated by the pivotal role of CXCR4 as an HIV entry coreceptor, we herein report a *de novo* hit-to-lead effort on the identification of subnanomolar purine-based CXCR4 antagonists against HIV-1 infection. Compound **24**, with an EC_{50} of 0.5 nM against HIV-1 entry into host cells and an IC_{50} of 16.4 nM for inhibition of radioligand stromal-derived factor-1α (SDF-1α) binding to CXCR4, was also found to be highly selective against closely related chemokine receptors. We rationalized that compound **24** complementarily interacted with the critical CXCR4 residues that are essential for binding to HIV-1 gp120 V3 loop and subsequent viral entry. Compared to the marketed CXCR4 antagonist AMD3100 (Plerixafor), compound **24** showed a 130-fold increase in anti-HIV activities, while both compounds only exhibited similar potency in mobilization of CXCR4+/CD34+ stem cells at a high dose. Our study offers insights for anti-HIV therapeutic design to be devoid of major interferences with SDF-1α function.

INTRODUCTION

The battle against HIV/AIDS remains a formidable task and is of paramount importance to develop efficacious therapies with minimal resistance. With significant progress in elucidating molecular insights into HIV pathogenesis and druggable targets, the Highly Active Antiretroviral Therapy (HAART) arsenal has evolved beyond the traditional drugs that target three main viral enzymes: reverse transcriptase, integrase and protease.[1, 2] In particular, the HIV entry mechanism involving multiple conformational changes has provided potential targets and propelled a plethora of therapeutic developments for the disruption of HIV viral attachment, coreceptor binding and fusion.[3-8] HIV-1 infection is initiated by the association of viral glycoprotein 120 (gp120) with CD4 cell receptor, which in turn triggers a conformational change in gp120, allowing exposure of the third variable loop (V3 loop) of gp120 to bind to the chemokine receptors including T cell-tropic CXCR4 or macrophage-tropic CCR5. The subsequent conformational change in gp41 leads to a fusion of the viral envelope and host cell membrane.[9] Indeed, enfuvirtide, a peptidomimetic of gp41, was approved by FDA in 2003 to block HIV-1 viral fusion.[10, 11] A decade after uncovering the critical roles of chemokine receptors CXCR4 and CCR5 in mediating HIV entry, the first-in-class CCR5 chemokine receptor antagonist maraviroc was approved in 2007 to provide additional anti-HIV treatment arsenal.[12] The clinical observation of the predominant CXCR4-utilizing strains in HIV-1 infected patients after maraviroc administration[13] suggests a mixed-tropic viral population and thus a necessity in the development of CXCR4 antagonists for complete viral suppression.

The induced chemotactic signaling mediated by the chemokine SDF-1α (also known as C-X-C motif chemokine 12α, CXCL12α) and its receptor CXCR4 is of significant biological importance involved in tumor metastasis, angiogenesis, tumor progression and survival.[14-16] Interestingly, this pathway is also exploited by pathogens to alter the signaling patterns of the hosts in various disease progressions.[17, 18] The imperative need for selective CXCR4 antagonists is not limited to therapeutic applications in blocking HIV-1 entry, but also in modulating SDF-1α:CXCR4 axis' involvement in tumor metastasis, angiogenesis, tumor progression and survival.[14-16] Notably, in about 50% of the late

stage HIV-1 infected patients, HIV-1 used either CXCR4 alone or in combination with CCR5 to facilitate viral entry into host cells and accelerate disease progression.[19] The emergence of CXCR4-utilizing strains also coincides with the onset of immune deficiency accompanying by a marked drop of CD4+ T-cell counts, thereby facilitating HIV-1 replication.[20-22] It was shown that SDF-1α, at low concentration, could effectively disrupt the association of HIV-1 with CXCR4 and therefore reduce the infection.[23-25] The disruption comes from the steric hindrance caused by the binding of SDF-1α to CXCR4. Furthermore, SDF-1α-mediated down regulation of cell-surface CXCR4 by inducing its endocytosis could lead to inhibition of HIV infection.[26] CXCR4 has been validated as a viable target in that the selective CXCR4 antagonists, such as AMD3100 (Plerixafor)[27], or oral-bioavailable AMD0070[28], could significantly reduce viral load in T-tropic (X4) HIV-infected patients. However, AMD3100 failed as an HIV drug in phase II clinical trials for lacking oral availability and cardiac disturbance.

The recently reported co-crystal structures of CXCR4 with its antagonists[29], IT1t, a small molecule, and CVX15, a cyclic peptide, have provided key design features for new compounds. Both SDF-1α and the V3 loop of HIV-1 gp120 complement a substantial portion of the CXCR4 acidic extracellular domain, forming multiple salt-bridge contacts with predominantly the aspartate and glutamate residues.[18, 29, 30] In turn, a myriad of highly basic CXCR4 antagonists were developed to exploit these charge-charge interactions as they play pivotal roles in binding to CXCR4 receptor.[31, 32] To identify efficacious agents against T-tropic (X4) HIV-1 infections, herein, from the discovery of quinazoline-based polyamine CXCR4 antagonists as HIV-1 entry inhibitors, we will describe the design, synthesis and structure-activity relationship (SAR) to culminate in a novel series of HIV-1 selective, CXCR4 specific, purine-based antagonists with a broad therapeutic window. Our study provides tantalizing insights into developing antagonists that selectively target key CXCR4 residues that govern the HIV-1 entry process.

Chemistry

Side chains **A-H** in Figure 1 and test compounds **1-8** in Table 1 were prepared according to a general synthetic route shown in previous literature.[33] Test Compounds **9-11** were prepared according to a general synthetic method shown in Scheme 1 using compound **Ia** and its corresponding 2,4-diamino quinazoline **9**, respectively, as a typical example. The commercially available 2-amino-5-methoxy benzoic acid (**Ia**) was coupled with urea to provide 6-methoxy-quinazoline-2,4-diol (**IIa**) in 85% yield. Treatment of **IIa** with phosphorus oxychloride in the presence of 2-ethyl-pyridine as a base gave 2,4-dichloro-6-methoxy-quinazoline (**IIIa**), which without purification was first coupled with 4-amino-1-Boc-piperidine in a chemoselective manner to give intermediate **IVa** in 59% yield over two steps, followed by a second coupling with protected side chain **D** under microwave irradiation to afford **Va** in 63% yield. Subsequent acidic deprotection afforded the desired compound **9** in 92% yield. Compounds **12-14** and **15-17** were synthesized respectively from **IVa-IVc** by coupling with side chains **E** and **F**, and deprotection with HCl/ether following a similar synthetic procedure for **Va** and **9**.

Test compounds **18** and **21-27** were prepared according to a general synthetic method shown in Scheme 2 using compound **18** as a typical example. The commercially available 2,6-dichloropurine was protected with 3,4-dihydro-2*H*-pyran to provide **18-I** in quantitative yield, which in turn was coupled with side chain **D** in a chemoselective manner to give intermediate **18-II** in 62% yield, followed by a second coupling with piperazine under microwave irradiation (15 min, 100 ^{o}C) or heating at 100 ^{o}C in 1-pentanol for 15 hours to afford **18-III** in 64% yield. After acidic deprotection, compound **18** was obtained in 94% yield. Compound **22** and **25-27** were synthesized respectively from **18-I** by coupling with different side chains followed by a second coupling with piperazine and deprotection with HCl/ether in a procedure similar to that for **18**. The synthesis of compound **19** was shown in scheme 3.

RESULTS AND DISCUSSION

Quinazoline-based antagonists.

Our group has previously reported a series of potent quinazoline-based CXCR4 antagonists on their abilities to mobilize stem cells.[33] In the present study, we evaluated the potential of these quinazoline-based CXCR4 antagonists (Table 1) in the blockade of HIV-1 entry by performing luciferase activity assays using TZM-bl cells (see Materials and Methods). The binding affinities of compounds **1**-**5** toward the CXCR4 receptor increased significantly by 10- to 20-fold through terminal ring-size expansion from three- to seven-membered ring, which also showed a relatively good correlation with their anti-HIV-1 activities. Despite the nitrogen atoms at the R^3 position of compounds **4**'s and **6**'s terminal six-membered rings displaying distinct binding modes towards CXCR4, they both harnessed similar CXCR4 binding affinities and anti-HIV-1 activities. Compounds **7** with a terminal piperazine ring and **8** with an exposed tertiary amine all showed dramatic decreases in CXCR4 binding and anti-HIV activities, suggesting a hydrophobic pocket existing in CXCR4 to facilitate the terminal binding of the antagonists.

We further addressed the influence of the quinazoline core in CXCR4 binding by synthesizing a series of compounds, **9-17**. We installed electron-donating methoxy group added either at the R^1 or R^2, or both R^1 and R^2 positions, in combination with modifications at the R^3 position by terminal cyclohexyl, cycloheptyl, or piperidine ring, respectively (Table 1). Compared to compound **4**, the addition of a methoxy group either at the R^1 or R^2 position led to a 4~5-fold moderate increase in CXCR4 binding affinity for both compounds **9** and **10** with terminal cyclohexyl ring and compounds **12** and **13** with cycloheptyl ring at the R^3 position. The terminal ring could situate in a hydrophobic cleft of CXCR4, and the mounting of a methoxy group to the quinazoline core might induce an allosteric conformational change of the compound to facilitate its interaction with CXCR4. Moreover, the increased electron density by the introduced methoxy group might play a role in the enhanced binding of the compound to CXCR4. However, double modifications at both the R^1 and R^2 positions with methoxy groups did not further increase, but only maintained (compound **11**), or even decreased (compounds **14** and **17**) the binding affinity of the compounds to CXCR4, suggesting that hydrophobic interactions could be involved for the binding. Moreover, the introduction of two methoxy groups could affect the binding orientations of the compounds by shifting the larger

cycloheptyl ring (compound **14**) out of position or extending the piperidine tertiary amine to an unfavourable binding mode (compound **17**). Interestingly, such effect was tolerated for compound **11** with the cyclohexyl ring, since the CXCR4 binding affinity was maintained.

Despite the strong CXCR4 bindings by compounds **9, 10, 12** and **13** (IC_{50} ~ 10 nM), only compound **10** with the terminal cyclohexyl ring showed a significant 8-fold increase in the blockade of HIV-1 infection (EC_{50} = 8.6 nM). The addition of a methoxy group at the R^2 position presumably allowed the cyclohexyl ring to adopt a favourable binding orientation, resulting in better interactions with key residue(s) on CXCR4 for HIV-1 entry. From the SAR studies, we identified that compound **10**, a quinazoline-based CXCR4 antagonist, had a higher CXCR4 binding affinity and potent anti-HIV activity when compared to the documented CXCR4 antagonists AMD3100 and IT1t (Table 1). However, with the exception of compound **4**, the quinazoline-based antagonists had moderate cytotoxicities to CEM and TZM-bl cells, and were deemed an appropriate replacement of the core and other functional groups. Taken together, we based the next design on an incorporation of a different core scaffold while maintained the terminal cyclohexyl ring on the projected arm.

Purine-based antagonists

In an effort to increase the therapeutic index of the CXCR4 antagonists and maintain the extended two-arm projections of the quinazoline-based structures, we employed purine as a new core and synthesized a series of potent CXCR4 antagonists, **18-27** (Table 2). Gratifyingly, there was a significant increase of the therapeutic index as many of the purine-based antagonists exhibited no toxicities at concentrations up to 50 μM in CEM and TZM-bl cells. With the purine scaffold, we first tested the effects of the side chain modifications. Compound **18A** was first synthesized to carry similar two side chains from compound **4**, however, its CXCR4 binding affinity was dramatically decreased to 230 nM (Figure 2). This is likely due to the loss of hydrophobic interactions of the purine scaffold to the CXCR4 cleft as compared to the quinazoline core. Surprisingly, the CXCR4 binding affinity of compound **18** was restored to 18.1 nM by swapping the orientations of the two side chains, and its potency of anti-HIV-1 activity was improved to 2.0 nM (Table 2). The binding orientation of

compound **18** may form strong interactions with residues in the extracellular domain of CXCR4 that are important for binding to the HIV-1 gp120 V3 loop.

The methyl group incorporation either at the R^1 position of the purine imidazole ring in compound **19** or at both the R^1 and piperazine ring-linked R^2 positions in compound **20** resulted in a 4~5-fold decrease in CXCR4 binding affinity. The potency of HIV-1 inhibition was generally maintained in the low nanomolar range with a 2-fold decrease in anti-HIV activity as compared to that of compound **18**. However, these methyl group modifications also led to unfavourable cytotoxicities. The maintaining of the anti-HIV activities for compounds **18-20** implied the importance of the orientation and binding modes of the two side chains. The elongation of the lower side chain by 4-methylpiperidine in compound **21** led to a 2~3-fold decrease in CXCR4 binding and yet a 40-fold decrease in anti-HIV activity (Table 2), suggesting a small binding pocket in the lower side chain that allows for limited substitutions.

We next turned our attention to the appropriate placement for the peripheral functionalities in the upper side chain of the purine-based antagonists. Compound **22** with a pyridine substitute of the phenyl ring moiety showed a 2-fold decrease in both CXCR4 binding and anti-HIV activities as compared to compound **18**, suggesting that the N atom in the pyridine ring might not significantly change the binding role of the original phenyl ring moiety (Table 2). To further access the possible binding motifs and to increase the anti-HIV activity, we investigated the effects of varying chain length by installing extra methylene groups at positions *n* and *m* of the upper functional chain (Table 2). With an introduced methylene group at position *n*, compound **23** showed an around 2-fold decrease in both CXCR4 binding and anti-HIV activities, suggesting that the orientation of the π-π stacking interactions arising from neighbouring aromatic rings might be important in CXCR4 binding. However, with the introduced methylene group at position *m*, compound **24** showed a 4-fold enhancement of anti-HIV activity (EC_{50} = 0.5 nM), while its CXCR4 binding affinity was not changed as compared to that of compound **18** (Table 2). The results suggested that the degree of rotation and flexibility of terminal chain from the *m* position allow particular interactions with residues on the CXCR4 receptor that can closely control HIV-1 entry. Encouraged by the above findings, we

envisioned that compound **25** with meta-substitution would harness similar projection of the peripheral upper side chain to that of compound **24**. Indeed, compound **25** exhibited a comparable anti-HIV activity to that of compound **24**, while there was a 4-fold increase in CXCR4 binding affinity. The less correlation between the CXCR4 binding affinity and anti-HIV activity for compounds **18, 24** and **25,** as an example**,** suggested that additional mechanisms are involved in determining the anti-HIV activity. As compared to compound **25**, compounds **26** and **27**, with the same projection of the peripheral upper side chain, exhibited a 4~10-fold decrease in both CXCR4 binding and anti-HIV activities, suggesting that the presence of a tertiary amine in the pyridine moiety would either hinder the π-π stacking interactions between neighbouring aromatic rings of the compound or interfere with the hydrophobic cleft of CXCR4. Interestingly, compounds **26** bearing a pyridine substitution and a meta-substitution of the peripheral upper side chain, showed similar CXCR4 binding and anti-HIV activities as compound **22**. The above findings implied that the projection of the meta-substituted upper side chain from a phenyl ring in compound **25** produced a favourable binding orientation with CXCR4.

In comparison to the initially quinazoline-based compound **4**, our hit-to-lead generation effort resulted in the identification of compound **24** with improved CXCR4 binding affinity and HIV-1 entry inhibition by 2.2-fold and 134-fold (Table 1 vs Table 2), respectively. Furthermore, we greatly reduced the cytotoxicities of the quinazoline-based CXCR4 antagonists by the substitution with a purine core. Intriguingly, compound **18A** with a purine core swapping of the quinazoline core in compound **4** resulted in a significant loss of CXCR4 binding. However, compound **18** with a switching of the two peripheral appendages in compound **18A** readily restored the CXCR4 binding activity. Moreover, such employment increased the anti-HIV-1 entry activity by 34.2-fold (Figure 2 vs Table 2). Taken together, from the SAR studies of the CXCR4 antagonists, we have shown: 1) the importance of a terminal cyclohexyl ring group; 2) the cytotoxic effects of the quinazoline core resolved by a purine core replacement; 3) the orientation of the side chains with projected peripheral functionalities involved in CXCR4 binding and anti-HIV activities and 4) the effects of hydrophobic interactions between the antagonists and CXCR4. Furthermore, the SAR studies could lead to the

exploration of other potential binding sites on the CXCR4 receptor for HIV-1 entry by introducing flexibility and optimization of the upper side chain of the purine-based antagonists.

Time of addition assays

To validate that these CXCR4 antagonists are HIV-1 entry inhibitors through interactions with CXCR4, we performed time of addition assays over one HIV replication cycle by monitoring the effects of compound **24** in TZM-bl cells. Compound **24**, at various concentrations ranging from 0 to 20 nM, was added three hours before, simultaneously with, and three hours after HIV-1 infection, and showed a dose-dependent inhibition of viral replication (Figure 3). When added three hours before or simultaneously with HIV-1 infection, compound **24** maintained its potent anti-HIV activities at EC_{50} concentrations consistent with the observation in Table 2. In contrast, the anti-HIV activity by compound **24** was significantly reduced, when added three hours after HIV-1 infection. The pre- and co-treatments with compound **24** in HIV-1 infection provided more protection than the post-treatment, confirming that the CXCR4 antagonist indeed protected against viral entry in the early phase of HIV-1 infection.

Molecular dynamics simulation study

We then carried out molecular dynamics (MD) simulations to investigate the interacting CXCR4 (PDB code 3OE0)[29] residues to gain insights into the possible binding mode of compound **24** (Figure 4 and Figure S1). Intriguingly, compound **24** docked towards the N-terminal domain of CXCR4 and formed hydrogen bonding with the CXCR4 residues Asp193, His281, and Glu288. As shown in Figure 4A, from purine core to lower piperazine ring of compound **24**, of which two hydrogen bonds formed with CXCR4: the N3 of the purine core interacting with the side chain of His281 and the terminal piperazine nitrogen with the side chain of Glu288. In particular, Glu288 of CXCR4 has been shown to be one of the most important residues for HIV-1 coreceptor activity. A significant loss (>50%) of this activity was observed by the substitution of Glu288 with either alanine or even aspartic acid that preserves the physicochemical properties.[34, 35] Moreover, the nitrogens from the projected upper side chain of compound **24** formed two hydrogen bonds with Asp193 side chain. From a simulation study, Asp193 is found to form a highly interacting salt bridge with V3 loop residue

Lys10.[30] Moreover, alanine substitution of Asp193 resulted in a dramatic reduction of the HIV-1 coreceptor activity of CXCR4.[36] While alanine substitutions at Asp187 and Phe189 of the CXCR4 residues also experimentally impaired >60% of the HIV-1 coreceptor activity, site directed mutagenesis studies demonstrated the crucial roles of Arg188, Tyr190, and Pro191 in HIV-1 binding.[35, 37-40] Interestingly, the terminal cyclohexyl ring and the upper side chain of compound **24** picked up several significant hydrophobic interactions with the CXCR4 residues Phe189, Tyr190 and Pro191. The phenyl ring moiety linked to the purine core in compound **24** was involved in hydrophobic interactions with Tyr190, Gln200 and Leu266. The alanine substitution of Gln200 was found to significantly affect HIV-1 coreceptor binding.[39] Moreover, Gln200 is calculated to form a strong nonpolar interaction with the aromatic ring of the V3 loop residue Trp20.[30] Taken together, the MD results provided great insight into the molecular interactions between compound **24** and CXCR4 receptor. We reasoned that the potent anti-HIV activity of compound **24** could come from its interactions with the critical CXCR4 residues in the N-terminal domain that are exploited by HIV-1 V3 loop for viral entry. To provide further insight into the potent HIV entry inhibition by these purine-based antagonists, compound **25** was subjected to MD study (Figure S2). Gratifyingly, compound **25**, similar to that of compound **24**, docked to the N-terminal extracellular loop II domain and interacted with majority of the abovementioned CXCR4 residues. MD simulations showed that compound **25** hydrogen bonded to several CXCR4 residues that were reported to be critical for HIV entry. By modifying the orientation of the upper side chain in compound **24** from *para* to *meta* in compound **25**, compound **25**'s upper side chain gained additional strong hydrogen bond interactions with Asp187, Glu277 and hydrophobic interaction with Arg188.[35, 37, 39] The terminal piperazine nitrogens of both compounds **24** and **25** were anchored towards the interior of CXCR4 by interacting with the side chain of Glu288, an important residue for HIV coreceptor activity. In all, by targeting a distinct domain of CXCR4 that could be pivotal for HIV-1 entry, we greatly improved the anti-HIV activities of compounds **24** and **25** to the subnanomolar range, a 130-fold enhancement in potency relative to that of AMD3100. Furthermore, we envisioned that a lower dose of compound **24** could be

employed for treatment of chronic HIV-1 infection to minimize adverse effects of normal physiological functions of SDF-1α:CXCR4 axis.

Binding specificity and functional activity tests

Since compounds **24** and **25** were identified with strong binding affinities for CXCR4 and potent anti-HIV entry activities in subnanomolar range, further studies were conducted to address their binding specificities and functional activities. As shown in Table 3, compounds **24** and **25** exhibited >609-fold and >2,380-fold selectivities for CXCR4 binding, respectively, versus a panel of closely related chemokine receptors including CXCR2, CCR2, CCR4 and CCR5 whose binding affinities were >10,000 nM (as IC_{50}). Furthermore, compounds **24** and **25** showed specific inhibitions for CXCR4. Recent reports had suggested that CXCR7 is the most closely-related chemokine receptor to CXCR4.[41] Using the established SDF-1α-dependent β-arrestin assay of CXCR7,[42] compound **24** did not antagonize SDF-1α binding to CXCR7 and the triggering of β-arrestin recruitment even at forty-fold higher SDF-1α concentration, providing a >1,960-fold functional selectivity over CXCR4-dependent HIV entry inhibition by compound **24** (Figure S3). These results, together with several reported CXCR4 antagonists,[31] strongly suggested that the introduction of nitrogen-containing appendages with a purine core or other skeletons might be pivotal in designing potent and specific CXCR4 antagonists. The nitrogen-containing fragments could mimic the Lys/Arg-rich nature of the SDF-1α, the natural ligand involved in the binding and activation of CXCR4.[43] Moreover, since TZM-bl cells express both CXCR4 and CCR5 coreceptors, the lack of binding of compounds **24** and **25** to CCR5 from the abovementioned results provided strong support that the observed potent anti-HIV entry effects (EC_{50} ~0.5 nM) were correlated with their binding to CXCR4 expressed on the TZM-bl cell surface.

Despite the significant therapeutic potential of SDF-1α in blocking CXCR4 in the HIV field, growing evidences have accumulated that SDF-1α:CXCR4 axis is involved in tumor progression, angiogenesis and metastasis.[14, 15] Recent findings have validated that cancer cells expressing CXCR4 are migrated to metastasis target tissues that release SDF-1α.[14, 15] A question concerning whether our newly developed CXCR4 antagonists overlapped with the SDF-1α binding sites on the CXCR4

receptor was raised. We addressed this issue by investigating the inhibitory activity of compound **24** on SDF-1α-induced cell migration. The chemotaxis inhibition assay was performed using CCRF-CEM cells that express endogenous human CXCR4. As shown in Figure 5A, while there was no apparent toxicities to CEM cells (CC_{50} > 50μM), compound **24** exerted an IC_{50} of 3.1 nM to block SDF-1α-induced CEM migration. This was fairly comparable to the IC_{50} (16.4 nM) for the inhibition of radioligand ^{125}I-SDF-1α binding by compound **24** to hCXCR4-transfected membrane (Table 2). AMD3100 was measured at 24.6 nM in this assay system. Thus, compound **24** was 8-fold more potent in CEM chemotaxis inhibition, and 13-fold more potent in CXCR4 binding than AMD3100 (Table 1 vs Table 2). Interestingly, the IC_{50} (213.1 nM) for 50% inhibition of ^{125}I-SDF-1α binding by AMD3100 to hCXCR4 (Table 1) was not comparable to its IC_{50} value for chemotaxis inhibition. This observation suggested that compound **24** might partially overlap with the SDF-1α binding sites on the CXCR4 receptor and that AMD3100 might access different binding sites.

Several observations on AMD3100's disruption of the homing of stem and progenitor cells had led to its serendipitous development as a mobilization agent of stem cells (CD34+). We were interested to find out if the significant increase of CXCR4 binding affinity by compound **24** would greatly enhance its mobilization abilities of stem cells. Using C57BL/6 mice for stem cell mobilization assay as previously described,[33] to our surprise, compound **24** was only found to mobilize CXCR4+/CD34+, the stem cells of interest, as efficiently as AMD3100 in the linear range (Figure 5B). CXCR4+/CD34+ cells were isolated in almost equal number from collected peripheral blood 2h after the indicated dosing (0.1 milligram per kilogram (mpk), 1 mpk and 5 mpk). Although compound **24** showed a 13-fold and 130-fold increase in CXCR4 binding affinity and anti-HIV-1 activity, respectively, it did not translate into an increased mobilization of stem cells. An explanation for this could be that compound **24** targeted residues of the distinct CXCR4 domains crucial for viral entry mediated by HIV-1 V3 loop since studies have shown that binding and signalling domains in CXCR4 are possibly distinct and separate.[30, 35, 37] This observation strongly suggested the decoupling of two CXCR4-mediated biological processes and the functional studies of compound **24** demonstrated the possibility of designing potent and selective CXCR4 antagonists.

CONCLUSION

In summary, we successfully designed and synthesized of a novel series of selective CXCR4 antagonists with a purine core scaffold that potently inhibited HIV-1 infection (**18-20** and **22-27**). Compound **24,** the most active inhibitor, displayed a strong binding affinity for CXCR4 (IC_{50} = 16.4 ± 3.5 nM) and a potent anti-HIV-1 activity as viral entry blocker (EC_{50} = 0.51 ± 0.02 nM), with no cytotoxicities up to 50 μM. Although more detailed structural studies are required to dissect the interactions between compound **24** and CXCR4, our MD simulations showed a high degree of molecular complementarity of compound **24** with CXCR4 residues essential for HIV-1 entry mediated by HIV-1 V3 loop. Compound **24**, when added prior to or simultaneously as in a time course experiment, showed potent inhibitions, confirming it as an HIV-1 entry inhibitor. Compared to AMD3100, the subnanomolar and function-oriented increase in HIV entry inhibition (>130-fold) of compound **24** should afford a significant dosage decrease in anti-HIV treatment. Since a much higher dose (5mpk) of compound **24** is needed to mobilize stem cells, the lower dosage of compound **24** may improve the therapeutic window of inhibiting HIV entry while reducing the disruption to stem cells homing in the bone marrow. Furthermore, these results strongly suggests that structural insights into the conformational states of CXCR4 towards compound **24** could aid future therapeutic design to minimize interference of normal physiological functions of SDF-1α:CXCR4 axis.

EXPERIMENTAL SECTION

General. Unless otherwise stated, all materials used were commercially obtained and used as supplied. Reactions requiring anhydrous conditions were performed in flame-dried glassware and cooled under an argon or nitrogen atmosphere. Unless otherwise stated, reactions were carried out under argon or nitrogen and monitored by analytical thin layer chromatography performed on glass-backed plates (5 × 10 cm) precoated with silica gel 60 F254 as supplied by Merck (Merck & Co., Inc., Whitehouse Station in Readington Township, NJ). Visualization of the resulting chromatograms was performed by looking under an ultraviolet lamp (λ = 254 nm) followed by dipping in an ethanol solution of vanillin (5% w/v) containing sulfuric acid (3% v/v) or phosphomolybdic acid (2.5% w/v)

and charring with a heat gun. Solvents for reactions were dried and distilled under an argon or nitrogen atmosphere prior to use as follows: THF, diethyl ether (ether), and DMF from a dark blue solution of sodium benzophenone ketyl; toluene, dichromethane, and pyridine from calcium hydride. Flash chromatography was used routinely for purification and separation of product mixtures using silica gel 60 of 230−400 mesh size as supplied by Merck. Eluent systems are given in volume/volume concentrations. Melting points were determined using a KRUSS KIP1N melting point meter. ^{1}H and ^{13}C NMR spectra were recorded on a Varian Mercury-300 (300 MHz) and a Varian Mercury-400 (400 MHz). Chloroform-d or dimethyl sulfoxide-d6 was used as the solvent and TMS (δ 0.00 ppm) as an internal standard. Chemical shift values are reported in ppm relative to the TMS in delta (δ) units. Multiplicities are recorded as s (singlet), br s (broad singlet), d (doublet), t (triplet), q (quartet), dd (doublet of doublets), dt (doublet of triplets), and m (multiplet). Coupling constants (J) are expressed in hertz. Electrospray mass spectra (ESMS) were recorded as *m/z* values using an Agilent 1100 MSD mass spectrometer. All test compounds displayed more than 95% purity as determined by Agilent 1100 series HPLC system using a C18 column (Thermo Golden, 4.6 mm × 250 mm). The gradient system for HPLC separation was composed of MeOH (mobile phase A) and H_2O solution containing 0.1% trifluoro-acetic acid (mobile phase B). The starting flow rate was 0.5 mL/min and the injection volume was 10 μL. During first 2 min the percentage of phase A was 10%. At 6 min, the percentage of phase A was increased to 50%. At 16 min, the percentage of phase A was increased to 90% over 9 min. The system was operated at 25 ^{o}C. Peaks were detected at 254 nm. IUPAC nomenclature of compounds was determined with ACD/Name Pro software.

***N*^{2}-{4-[(3-Cyclohexylamino-propylamino)-methyl]-benzyl}-6-methoxy-*N*^{4}-piperidin-4-yl-quinazoline-2,4-diamine hydrochloride salt (9).** To a magnetically stirred solution of **Va** (0.53 g, 0.64 mmole) in CH_2Cl_2 (10 mL) was added 1N HCl/diethylether (20 mL, 20 mmole) dropwise at 25 ^{o}C under an atmosphere of argon. The resulting mixture was stirred at 25 ^{o}C for 15 h and concentrated by removing the solvent to afford of compound **9** (0.38 g, 92%); ^{1}H NMR (300 MHz, D_2O) δ 7.56−7.50 (m, 4H), 7.15−6.93 (m, 3H), 4.71 (s, 2H), 4.26 (m, 2H), 4.24 (m, 1H), 3.73 (s, 3H), 3.51 (m, 2H), 3.20−3.05 (m, 6H), 2.13−1.70 (m, 10H), 1.56 (m, 1H), 1.33−1.11 (m, 6H); ^{13}C NMR (75 MHz,

D_2O) δ 158.69, 155.42, 151.48, 140.27, 132.41, 130.21, 129.52, 127.50, 124.55, 117.57, 108.96, 103.77, 57.33, 56.12, 50.61, 46.92, 44.02, 43.79, 43.18, 41.13, 28.72, 27.19, 24.32, 23.77, 22.75; ESMS *m/z*: 532.3 (M+1); HPLC purity = 95.35 %, tR = 14.35 min.

***N*^{2}-{4-[(3-Cyclohexylamino-propylamino)-methyl]-benzyl}-7-methoxy-*N*^{4}-piperidin-4-yl-quinazoline-2,4-diamine hydrochloride salt (10).** Compound **10** was synthesized from **Vb** (0.56 g, 0.67 mmol) following a similar synthetic procedure for **9** and obtained as a white solid (0.36 g, 83%); ^{1}H NMR (300 MHz, D_2O) δ 7.65 (d, *J* = 9.0 Hz, 1H), 7.55−7.48 (m, 4H), 6.50 (dd, *J* = 9.0, 2.1 Hz, 1H), 6.38 (d, *J* = 2.1 Hz, 1H), 4.67 (s, 2H), 4.26 (s, 2H), 4.21 (m, 1H), 3.74 (s, 3H), 3.53 (m, 2H), 3.17−3.01 (m, 6H), 2.13−1.71 (m, 10H), 1.56 (m, 1H), 1.33−1.13 (m, 6H); ^{13}C NMR (75 MHz, D_2O) δ 164.03, 158.85, 152.18, 140.29, 140.11, 130.20, 129.53, 127.53, 125.11, 113.62, 102.28, 97.72, 57.34, 55.96, 50.60, 46.78, 44.05, 43.75, 43.15, 41.15, 28.62, 27.33, 24.34, 23.77, 22.74; ESMS *m/z*: 532.3 (M+1); HPLC purity = 96.25 %, tR = 14.26 min.

***N*^{2}-{4-[(3-Cyclohexylamino-propylamino)-methyl]-benzyl}-6,7-dimethoxy-*N*^{4}-piperidin-4-yl-quinazoline-2,4-diamine hydrochloride salt (11).** Compound **11** was synthesized from **Vc** (0.53 g, 0.61 mmol) following a similar synthetic procedure for **9** and obtained as a white solid (0.37 g, 90%); ^{1}H NMR (300 MHz, D_2O) δ 7.57−7.48 (m, 4H), 7.26 (s, 1H), 6.65 (s, 1H), 4.75 (s, 2H), 4.26 (s, 2H), 4.23 (m, 1H), 3.83 (s, 6H), 3.48 (m, 2H), 3.19−3.00 (m, 6H), 2.13−1.96 (m, 6H), 1.93−1.71 (m, 4H), 1.65 (m, 1H), 1.33−1.13 (m, 6H); ^{13}C NMR (75 MHz, D_2O) δ 158.55, 154.62, 151.75, 146.11, 140.12, 134.66, 130.15, 129.39, 127.30, 103.61, 101.54, 97.33, 57.38, 56.40, 56.22, 50.67, 46.89, 44.03, 43.92, 43.19, 41.18, 28.69, 27.34, 24.33, 23.78, 22.78; ESMS *m/z*: 562.3 (M+1); HPLC purity = 95.27 %, tR = 14.23 min.

***N*^{2}-{4-[(3-Cycloheptylamino-propylamino)-methyl]-benzyl}-6-methoxy-*N*^{4}-piperidin-4-yl-quinazoline-2,4-diamine hydrochloride salt (12).** Compound **12** was synthesized from **IVa** by coupling with side chain **E** and deprotection with HCl/diethylether following a similar synthetic procedure for **9** and obtained as a white solid (0.37 g, 56% over 2 steps); ^{1}H NMR (300 MHz, D_2O) δ 7.56−7.50 (m, 4H), 7.14 (d, *J* = 2.1 Hz, 1H), 7.06 (dd, *J* = 9.3, 2.1 Hz, 1H), 6.94 (d, *J* = 9.3 Hz, 1H),, 4.71 (s, 2H), 4.26 (m, 2H), 4.24 (m, 1H), 3.72 (s, 3H), 3.53 (m, 2H), 3.20−2.96 (m, 6H), 2.13−1.80 (m,

9H), 1.68−1.31 (m, 10H); ^{13}C NMR(75 MHz, D_2O) δ 158.75, 155.47, 151.61, 140.30, 132.50, 130.23, 129.35, 127.58, 124.61, 117.65, 109.08, 103.81, 59.59, 56.15, 50.59, 46.93, 44.02, 43.70, 43.19, 41.58, 30.20, 27.22, 27.12, 23.12, 22.77; ESMS *m/z*: 546.4 (M+1); HPLC purity = 95.36 %, tR = 15.00 min.

***N*^{2}-{4-[(3-Cycloheptylamino-propylamino)-methyl]-benzyl}-7-methoxy-*N*^{4}-piperidin-4-yl-quinazoline-2,4-diamine hydrochloride salt (13).** Compound **13** was synthesized from **IVb** by coupling with side chain **E** and deprotection with HCl/diethylether following a similar synthetic procedure for **9** and obtained as a white solid (0.36 g, 57% over 2 steps); ^{1}H NMR (300 MHz, D_2O) δ 7.89 (d, *J* = 9.0 Hz, 1H), 7.55−7.49 (m, 4H), 6.94 (dd, *J* = 9.0, 2.1 Hz, 1H), 6.82 (d, *J* = 2.1 Hz, 1H), 4.78 (s, 2H), 4.35 (m, 1H), 4.26 (s, 2H), 3.91 (s, 3H), 3.47 (m, 2H), 3.17−2.99 (m, 6H), 2.13−1.77 (m, 7H), 1.90−1.39 (m, 12H); ^{13}C NMR (75 MHz, D_2O) δ 164.04, 158.87, 152.19, 140.34, 140.12, 130.23, 129.36, 127.63, 125.16, 113.63, 102.32, 97.73, 59.59, 55.97, 50.67, 46.78, 44.05, 43.65, 43.16, 41.58, 30.20, 27.36, 27.11, 23.13, 22.77; ESMS *m/z*: 546.4 (M+1); HPLC purity = 96.98 %, tR = 15.07 min.

***N*^{2}-{4-[(3-Cycloheptylamino-propylamino)-methyl]-benzyl}-6,7-methoxy-*N*^{4}-piperidin-4-yl-quinazoline-2,4-diamine hydrochloride salt (14).** Compound **14** was synthesized from **IVc** by coupling with side chain **E** and deprotection with HCl/diethylether following a similar synthetic procedure for **9** and obtained as a white solid (0.36 g, 52% over 2 steps); ^{1}H NMR (400 MHz, D_2O) δ 7.54−7.49 (m, 4H), 7.22 (s, 1H), 6.58 (s, 1H), 4.73 (s, 2H), 4.25 (s, 2H), 4.24 (m, 1H), 3.80 (s, 6H), 3.48 (m, 2H), 3.23−3.00 (m, 6H), 2.14−1.96 (m, 7H), 1.93−1.77 (m, 2H), 1.71−1.59 (m, 2H), 1.55−1.37 (m, 8H); ^{13}C NMR (75 MHz, D_2O) δ 160.99, 157.14, 154.21, 148.56, 142.75, 137.13, 132.75, 131.95, 129.92, 105.68, 103.95, 99.80, 62.20, 59.02, 58.82, 53.20, 49.47, 46.61, 46.46, 45.79, 44.22, 32.81, 29.94, 29.70, 25.70, 25.39; ESMS *m/z*: 576.4 (M+1); HPLC purity = 95.59 %, tR = 14.80 min.

6-Methoxy-*N*^{4}-piperidin-4-yl-*N*^{2}-{4-[(3-piperidin-1-yl-propylamino)-methyl]-benzyl}-quinazoline-2,4-diamine hydrochloride salt (15). Compound **15** was synthesized from **IVa** by coupling with side chain **F** and deprotection with HCl/diethylether following a similar synthetic procedure for **9** and obtained as a white solid (0.33 g, 51% over 2 steps); ^{1}H NMR (300 MHz, D_2O) δ 7.57−7.52 (m, 4H), 7.31 (s, 1H), 7.23−7.21 (m, 2H), 4.75 (s, 2H), 4.29 (m, 1H), 4.27 (s, 2H), 3.82 (s,

3H), 3.56−3.47 (m, 4H), 3.20−2.92 (m, 8H), 2.20−2.10 (m, 2H), 2.05−1.65 (m, 9H), 1.47 (m, 1H); ^{13}C NMR (75 MHz, D_2O) δ 158.70, 155.45, 151.50, 140.24, 132.40, 130.20, 129.48, 127.40, 124.56, 117.54, 108.99, 103.80, 61.61, 56.18, 53.29, 50.74, 46.96, 44.05, 44.00, 43.22, 27.21, 22.71, 20.97, 20.69; ESMS *m/z*: 518.3 (M+1); HPLC purity = 96.36 %, tR = 13.88 min.

7-Methoxy-*N*^{4}-piperidin-4-yl-*N*^{2}-{4-[(3-piperidin-1-yl-propylamino)-methyl]-benzyl}-quinazoline-2,4-diamine hydrochloride salt (16). Compound **16** was synthesized from **IVb** by coupling with side chain **F** and deprotection with HCl/diethylether following a similar synthetic procedure for **9** and obtained as a white solid (0.31 g, 49% over 2 steps); ^{1}H NMR (300 MHz, D_2O) δ 7.66 (d, *J* = 9.0 Hz, 1H), 7.57−7.51 (m, 4H), 6.17 (dd, *J* = 9.0, 2.1 Hz, 1H), 6.37 (d, *J* = 2.1 Hz, 1H), 4.66 (s, 2H), 4.27 (s, 2H), 4.21 (m, 1H), 3.70 (s, 3H), 3.56−3.51 (m, 4H), 3.23−2.91 (m, 8H), 2.27−2.20 (m, 2H), 2.05−1.65 (m, 9H), 1.49 (m, 1H); ^{13}C NMR (75 MHz, D_2O) δ 164.06, 158.81, 152.19, 140.24, 140.06, 130.18, 129.46, 127.82, 125.14, 113.66, 102.25, 97.73, 61.59, 55.97, 53.33, 53.29, 50.72, 44.06, 44.00, 43.18, 27.33, 22.72, 20.97, 20.69; ESMS *m/z*: 518.3 (M+1); HPLC purity = 99.05 %, tR = 12.73 min.

6,7-Dimethoxy-*N*^{4}-piperidin-4-yl-*N*^{2}-{4-[(3-piperidin-1-yl-propylamino)-methyl]-benzyl}-quinazoline-2,4-diamine hydrochloride salt (17). Compound **17** was synthesized from **IVc** by coupling with side chain **F** and deprotection with HCl/diethylether following a similar synthetic procedure for **9** and obtained as a white solid (0.32 g, 45% over 2 steps); ^{1}H NMR (400 MHz, D_2O) δ 7.54−7.44 (m, 4H), 7.29 (s, 1H), 6.68 (s, 1H), 4.76 (s, 2H), 4.35 (m, 1H), 4.27 (s, 2H), 3.86 (s, 6H), 3.57−3.49 (m, 4H), 3.25−3.16 (m, 4H), 3.10−2.91 (m, 4H), 2.27−2.20 (m, 2H), 2.05−1.65 (m, 9H), 1.51 (m, 1H); ^{13}C NMR (75 MHz, D_2O) δ 158.49, 154.61, 151.71, 146.01, 140.06, 134.60, 130.15, 129.43, 127.25, 103.13, 101.45, 97.27, 57.35, 56.43, 56.23, 53.30, 50.72, 46.92, 44.08, 44.02, 43.22, 27.35, 22.72, 20.95, 20.68; ESMS *m/z*: 548.3 (M+1); HPLC purity = 95.99 %, tR = 13.84 min.

***N*-Cyclohexyl-*N'*-{4-[(2-piperazin-1-yl-9*H*-purin-6-ylamino)-methyl]-benzyl}-propane-1,3-diamine hydrochloride salt (18).** A solution of 1N HCl/diethyl ether (4.8 mL) was added to the solution of **18-III** (240 mg, 0.31 mmole) in CH_2Cl_2 (9.6 mL). The reaction mixture was stirred for 15 hours and concentrated by removing the solvent to afford of compound **18** (174 mg, y: 94%); ^{1}H

NMR (400 MHz, D_2O) δ 8.40 (s, 1H), 7.52−7.44 (m, 4H), 4.82 (s, 2H), 4.26 (s, 2H), 4.01 (m, 4H), 3.29 (m, 4H), 3.21−3.08 (m, 4H), 2.18−2.02 (m, 4H), 1.82 (m, 2H), 1.63 (m, 1H), 1.40−1.12 (m, 6H); ^{13}C NMR (75 MHz, D_2O) δ 154.39, 151.63, 147.61, 139.56, 139.26, 130.13, 129.51, 127.95, 105.36, 57.39, 50.78, 44.06, 43.99, 42.56, 41.73, 41.20, 28.73, 24.37, 23.79, 22.77; ESMS *m/z*: 478.3 (M+1); HPLC purity = 96.8 %, tR = 13.07 min.

***N*-Cyclohexyl-*N'*-{4-[(9-methyl-2-piperazin-1-yl-9*H*-purin-6-ylamino)-methyl]-benzyl}-propane-1,3-diamine hydrochloride salt (19).** A solution of 1N HCl/diethyl ether (3 mL) was added to the solution of **19-III** (156 mg, 0.23 mmole) in CH_2Cl_2 (6 mL). The reaction mixture was stirred at 25 ^{o}C for 15h and concentrated by removing the solvent to afford **19** (123 mg, y: 91%),^{1}H NMR (400 MHz, D_2O) δ 8.75 (s, 1H), 7.55−7.45 (m, 4H), 4.82 (s, 2H), 4.27 (s, 2H), 4.04 (m, 4H), 3.85 (s, 3H), 3.26−3.11 (m, 8H), 2.18−2.04 (m, 4H), 1.84 (m, 2H), 1.66 (m, 1H), 1.40−1.12 (m, 6H); ^{13}C NMR (75 MHz, D_2O) δ 159.02, 151.60, 149.92, 140.24, 137.51, 130.12, 129.40, 127.95, 104.67, 57.42, 50.83, 44.00, 43.91, 42.83, 41.38, 41.24, 30.78, 28.78, 24.40, 23.84, 22.80; ESMS *m/z*: 492.3 (M+1); HPLC purity = 97.1 %, tR = 13.34 min.

***N*-Cyclohexyl-*N'*-(4-{[9-methyl-2-(4-methyl-piperazin-1-yl)-*9H*-purin-6-ylamino]-methyl}-benzyl)-propane-1,3-diamine hydrochloride salt (20).** Compound **20** was synthesized from **19-II** following a similar synthetic procedure for **19** with two steps and obtained as a white solid (143 mg, 65% over 2 steps); ^{1}H NMR (400 MHz, D_2O) 8.75 (s, 1H), 7.53 (d, *J* = 7.2 Hz, 2H), 7.48 (d, *J* = 7.2 Hz, 2H), 4.82 (s, 2H), 4.27 (s, 2H), 3.85 (s, 3H), 3.54 (m, 2H), 3.33 (m, 2H), 3.22−3.08 (m, 6H), 3.01 (m, 2H), 2.92 (s, 3H), 2.18−2.04 (m, 4H), 1.85 (m, 2H), 1.66 (m, 1H), 1.40−1.12 (m, 6H); ^{13}C NMR (75 MHz, D_2O) δ 159.49, 152.14, 150.30, 140.74, 137.95, 130.58, 129.85, 128.38, 105.21, 57.88, 53.25, 51.27, 44.45, 44.32, 43.38, 42.17, 41.67, 31.22, 29.22, 24.86, 24.28, 23.24; ESMS *m/z*: 506.3 (M+1); HPLC purity = 97.0 %, tR = 13.39 min.

***N*-{4-[(2-[4,4']Bipiperidinyl-1-yl-*9H*-purin-6-ylamino)-methyl]-benzyl}-*N'*-cyclohexyl-propane-1,3-diamine hydrochloride salt (21).** Compound **21** was synthesized from **18-I** following a similar synthetic procedure for **18** with three steps and obtained as a white solid (186 mg, 36% over 3 steps); ^{1}H NMR (400 MHz, D_2O) δ 8.06 (s, 1H), 7.52−7.44 (m, 4H), 4.82 (s, 2H), 4.34 (m, 2H), 4.25

(s, 2H), 3.46 (m, 2H), 3.22−2.90 (m, 8H), 2.18−1.76 (m, 10H), 1.65 (m, 1H), 1.61−1.10 (m, 12H); ^{13}C NMR (75 MHz, D_2O) δ 152.01, 151.05, 146.37, 140.88, 139.51, 130.17, 129.54, 128.18, 105.98, 57.39, 50.77, 46.66, 45.70, 44.17, 43.96, 41.19, 39.19, 37.59, 28.75, 27.99, 25.58, 24.39, 23.81, 22.77; ESMS *m/z*: 560.4 (M+1); HPLC purity = 99.3 %, tR = 13.69 min.

***N*-Cyclohexyl-*N'*-{6-[(2-piperazin-1-yl-*9H*-purin-6-ylamino)-methyl]-pyridin-3-ylmethyl}-propane-1,3-diamine hydrochloride salt (22).** Compound **22** was synthesized from **18-I** following a similar synthetic procedure for **18** with three steps and obtained as a white solid (150 mg, 29% over 3 steps); ^{1}H NMR (400 MHz, D_2O) δ 8.91 (s, 1H), 8.72−7.64 (m, 2H), 8.17 (d, *J* = 8.4 Hz, 1H), 5.27 (s, 2H), 4.57 (s, 2H), 3.93 (m, 4H), 3.39−3.12 (m, 8H), 2.24−2.06 (m, 4H), 1.86 (m, 2H), 1.68 (m, 1H), 1.42−1.18 (m, 6H); ^{13}C NMR (75 MHz, D_2O) δ 156.44, 155.40, 151.71, 149.16, 147.43, 143.02, 138.67, 129.21, 125.82, 105.08, 57.50, 47.19, 44.95, 42.64, 42.48, 41.38, 41.19, 28.80, 24.42, 23.84, 22.86; ESMS *m/z*: 479.3 (M+1); HPLC purity =98.6 %, tR = 13.69 min.

***N*-Cyclohexyl-*N'*-{4-[2-(2-piperazin-1-yl-*9H*-purin-6-ylamino)-ethyl]-benzyl}-propane-1,3-diamine hydrochloride salt (23).** Compound **23** was synthesized from **18-I** following a similar synthetic procedure for **18** with three steps and obtained as a white solid (197 mg, 38% over 3 steps); ^{1}H NMR (400 MHz, D_2O) δ 8.28 (s, 1H), 7.41−7.38 (m, 4H), 4.23 (s, 2H), 4.06 (m, 4H), 3.93 (s, 2H), 3.40 (m, 4H), 3.21−3.03 (m, 6H), 2.16−2.04 (m, 4H), 1.83 (m, 2H), 1.64 (m, 1H), 1.40−1.12 (m, 6H); ^{13}C NMR (75 MHz, D_2O) δ 154.29, 152.14, 147.64, 140.88, 139.31, 129.86, 129.80, 128.44, 105.93, 57.38, 50.79, 43.83, 43.55, 41.67, 41.43, 41.16, 34.32, 28.73, 24.37, 23.79, 22.75; ESMS *m/z*: 492.3 (M+1); HPLC purity = 95.4 %, tR = 13.31 min.

***N*-Cyclohexyl-*N'*-(2-{4-[(2-piperazin-1-yl-*9H*-purin-6-ylamino)-methyl]-phenyl}-ethyl)-propane-1,3-diamine hydrochloride salt (24).** Compound **24** was synthesized from **18-I** following a similar synthetic procedure for **18** with three steps and obtained as a white solid (195 mg, 38% over 3 steps); ^{1}H NMR (400 MHz, D_2O) δ 8.39 (s, 1H), 7.41 (d, *J* = 8.1 Hz, 2H), 7.32 (d, *J* = 8.1 Hz, 2H), 4.72 (s, 2H), 4.03 (m, 4H), 3.39−3.24 (m, 6H), 3.23−3.08 (m, 4H), 3.02 (m, 2H), 2.18−2.06 (m, 4H), 1.83 (m, 2H), 1.64 (m, 1H), 1.41−1.12 (m, 6H); ^{13}C NMR (75 MHz, D_2O) δ 154.21, 151.36, 147.53,

139.24, 136.81, 135.45, 129.05, 127.91, 105.19, 57.43, 48.57, 44.49, 44.13, 42.58, 41.75, 41.23, 31.25, 28.76, 24.40, 23.82, 22.77; ESMS *m/z*: 492.3 (M+1); HPLC purity = 99.6 %, tR = 13.34 min.

***N*-Cyclohexyl-*N'*-{3-[(2-piperazin-1-yl-*9H*-purin-6-ylamino)-methyl]-benzyl}-propane-1,3-diamine hydrochloride salt (25).** Compound **25** was synthesized from **18-I** following a similar synthetic procedure for **18** with three steps and obtained as a white solid (178 mg, 34% over 3 steps); ^{1}H NMR (400 MHz, D_2O) δ 8.34 (s, 1H), 7.52−7.36 (m, 4H), 4.82 (s, 2H), 4.21 (s, 2H), 3.99 (m, 4H), 3.27 (m, 4H), 3.21−3.09 (m, 4H), 2.18−2.02 (m, 4H), 1.81 (m, 2H), 1.63 (m, 1H), 1.40−1.12 (m, 6H); ^{13}C NMR (75 MHz, D_2O) δ 154.40, 151.56, 147.74, 139.30, 139.01, 130.92, 129.54, 128.81, 128.55, 128.40, 105.37, 57.44, 51.04, 44.20, 44.11, 42.60, 41.77, 41.25, 28.78, 24.42, 23.84, 22.81; ESMS *m/z*: 478.3 (M+1); HPLC purity = 95.3 %, tR = 13.30 min.

***N*-Cyclohexyl-*N'*-{6-[(2-piperazin-1-yl-*9H*-purin-6-ylamino)-methyl]-pyridin-2-ylmethyl}-propane-1,3-diamine hydrochloride salt (26).** Compound **26** was synthesized from **18-I** following a similar synthetic procedure for **18** with three steps and obtained as a white solid (152 mg, 30% over 3 steps); ^{1}H NMR (400 MHz, D_2O) δ 8.49 (s, 1H), 8.04 (t, *J* = 7.6 Hz, 1H), 7.63 (d, *J* = 7.6 Hz, 1H), 7.58 (d, *J* = 7.6 Hz, 1H), 4.98 (s, 2H), 4.47 (s, 2H), 3.92 (m, 4H), 3.24−3.10 (m, 6H), 3.08 (m, 2H), 2.18−2.02 (m, 4H), 1.77 (m, 2H), 1.60 (m, 1H), 1.36−1.08 (m, 6H); ^{13}C NMR (75 MHz, D_2O) δ 156.81, 155.07, 151.68, 148.50, 148.15, 141.16, 139.04, 123.50, 123.16, 105.30, 57.44, 49.90, 44.89, 44.63, 42.57, 41.61, 41.19, 28.75, 24.37, 23.81, 22.77; ESMS *m/z*: 479.3 (M+1); HPLC purity = 98.5 %, tR = 13.11 min.

***N*-Cyclohexyl-*N'*-{5-[(2-piperazin-1-yl-*9H*-purin-6-ylamino)-methyl]-pyridin-3-ylmethyl}-propane-1,3-diamine hydrochloride salt (27).** Compound **27** was synthesized from **18-I** following a similar synthetic procedure for **18** with three steps and obtained as a white solid (154 mg, 30% over 3 steps); ^{1}H NMR (400 MHz, D_2O) δ 8.96−8.93 (m, 2H), 8.79 (s, 1H), 8.56 (s, 1H), 5.14 (s, 2H), 4.57 (s, 2H), 4.02 (m, 4H), 3.38−3.26 (m, 6H), 3.10 (m, 2H), 2.23−2.06 (m, 4H), 1.84 (m, 2H), 1.67 (m, 1H), 1.40−1.15 (m, 6H); ^{13}C NMR (75 MHz, D_2O) δ 156.26, 152.33, 149.09, 148.44, 142.15, 141.80, 140.20, 139.39, 131.28, 105.92, 57.93, 47.77, 45.42, 43.18, 41.99, 41.62, 41.51, 29.22, 24.86, 24.28, 23.29; ESMS *m/z*: 479.3 (M+1); HPLC purity = 99.0 %, tR = 12.98 min.

Establishment of Human CXCR4 Stable Cell Line and Membrane Purification. The hCXCR4 cDNA was subcloned into pIRES2-EGFP vector (Clontech Laboratories, Inc., Mountain View, CA). Transfected HEK-293 cells stably expressed hCXCR4 (HEK-293 CXCR4) were selected by EGFP and 1 mg/ml G418 sulfate. The selected clone was maintained in DMEM supplemented with 10% fetal bovine serum and 0.5 mg/ml G418 sulfate with 5% CO_2 at 37°C in the humidified incubator. For membrane purification, cells were homogenized in ice-cold buffer A (50 mM Tris-HCl, pH 7.4, 5 mM $MgCl_2$, 2.5 mM EDTA, 10% sucrose) with freshly prepared 1 mM PMSF. The homogenate was centrifuged at 3500 x g for 15 min at 4°C. The pellet was removed and the supernatant then was centrifuged at 43000 x g for additional 30 min at 4°C. The final pellet was resuspended in buffer A and stored at -80°C.

Radioligand Binding Assay. An amount of 2-4 μg of purified membrane with CXCR4 was incubated with 0.16 nM ^{125}I-SDF-1α and compounds of interest in the incubation buffer (50 mM HEPES-NaOH, pH 7.4, 100 mM NaCl, 5 mM $MgCl_2$, 1 mM $CaCl_2$, 0.5% BSA) The nonspecific binding was defined in the presence of 50 μM AMD3100 (plerixafor). The reaction mixtures were incubated for 1.5 h at 30°C and then transferred to a 96-well GF/B filter plate (Millipore Corp., Billerica, MA). The reaction mixtures were terminated by manifold filtration and washed with ice-cold wash buffer (50 mM HEPES-NaOH, pH 7.4, 100 mM NaCl) for four times. The radioactivity bound to the filter was measured by Topcount (PerkinElmer Inc., Waltham, MA). IC_{50} values were determined by the concentrations of compounds required to inhibit 50% of the specific binding of ^{125}I-SDF-1α and calculated by nonlinear regression (GraphPad software, San Diego, CA).

Luciferase Activity Assay. Using TZM-bl cells, the luciferase activity assays were performed for studying the efficacy of the CXCR4 antagonists on HIV-1 infectivity. TZM-bl is a HeLa-derived cell line expressing high levels of the introduced CD4, CCR5 and CXCR4 receptors, and contains HIV-1 long terminal repeat-driven β−galactosidase and luciferase reporter cassettes that are activated by HIV-1 Tat expression.[44] For the luciferase reporter experiments, 5×10^3 cells/well were plated in 96-well plates and cultured at 37°C with 5% CO_2 in the humidified incubator. After one or two overnight incubation and usually 30 min prior to HIV infection, TZM-bl cells were treated with CXCR4

antagonists in serial dilution and then infected by HIV-1IIIB at a multiplicity of infection (M.O.I.) of 1. The HIV-1 IIIB strain was used for infection. FARCyte machine (Amersham Pharmacia) was used for data reading and at least three independent experiments were carried out to get the standard deviation.

Cytotoxicity Assay. CEM, a human T-lymphoblast leukemia, and TZM-bl cells were used for cell cytotoxicity assays. 1×10^4 cells/well were plated in 24-well plates. After overnight incubation, cells were treated with CXCR4 antagonists for 72 hours. The cells were then fixed and stained with 0.5% methylene blue in 50% ethanol for 2 hours at room temperature, followed by washing with tap water to remove excess color. Plates were dried, then resuspended in 1% sarkosyl and incubated for 3 hrs at room temperature. Methylene blue was oxidized by living cells to a colorless product, while dead cells remained blue colored. Cell growth was quantitated based on the amount of methylene blue adsorbed into cells measured by a spectrophotometer (Molecular Devices) at 595 nm. All experiments were performed in triplicate wells and repeated at least three times to get the standard deviation.

Docking analysis of compounds with CXCR4. The protein structures of CXCR4 (Protein Data Bank identifier [PDB ID] no. 3OE0)[29] was applied for this study. All the calculations were performed using Discovery Studio 2.1 (DS 2.1) (Accelrys, Inc., San Diego, CA). The docking analysis was conducted using the DS/LigandFit program with the CHARMm force field.[45] The number of docking poses was set as 100 with default parameters. The decision of the best pose was according the binding information from the Wu et al.[29]

Molecular dynamics simulations. The molecular dynamics (MD) simulations were carried out using GROMACS v4.5.4 to refine the docked structures.[46, 47] The topology of docked ligand was generated by PRODRG serve.[48] The force field for the whole system was GROMOS 43a1.[49] The protein-ligand complex was restrained in a box of cubic shape whose edges were placed at 1 nm from the complex and SPC/E water model was performed. The system was electrically neutralized by adding 11 Cl^- ion. A two-step energy minimization was performed using steepest descent and conjugate gradient algorithms to converge the system upto 10 kJ $mol^{-1}nm^{-1}$. After a short energy minimization step, the system was subjected to NVT (300K) and NPT (1 bar) equilibration with 100

ps running, and LINCS algorithm was used to constrain the hydrogen bond lengths.[50] The time step was kept at 2 fs for the simulation. The cut-off distance of 10 Å was used for all short range non-bonded interactions and 12 Å Fourier grid spacing in PME method for long range electrostatics. Finally the restraints of complex structure were removed and performed to a 20 ns MD calculation (Supporting Information 1).

Chemotaxis Assay. CCRF-CEM (T-cell acute lymphoblastic leukemia) cells were suspended in RPMI 1640 containing 10% FBS and then preincubated with indicated concentrations of compounds for 10 min at 37 ^{o}C. The assay was performed in Millicell Hanging Cell Culture Inserts (pore size 5 μm; 24-well plate; Millipore, Bedford, MA, USA). Compounds containing 10 nM SDF-1 were plated in the lower chambers of inserts, and cells with compounds were plated in the upper chamber of inserts at a density of 2.5×10^5 cells/well. After 2.5 h incubation at 37 ^{o}C, cells in both chambers of inserts were measured by flow cytometer (Guava Technologies, Hayward, CA, USA).

Flow Cytometry Analysis for Stem/progenitor cell counting. C57BL/6 male mice were treated with potential CXCR4 antagonist individually by subcutaneous injection, and then blood samples containing mobilized stem/progenitor cells were collected 2 hours later. After labeled with specific antibodies, including APC-conjugated anti-CXCR4 (clone 2B11; eBioscience), FITC-conjugated anti-CD34 (clone RAM34; eBioscience), PE-conjugated anti-CD133 (clone 13A4; eBioscience) and anti-KDR (clone Avsa12a1; eBioscience), anti-c-Kit (clone 2B8; eBioscience), anti-Sca-1 (clone D7; eBioscience), anti-linage (Mouse Hematopoietic Lineage Biotin Panel, eBioscience) and Streptavidin PE-Cy7 (eBioscience), cells were washed, characterized and quantified by flow cytometer (Guava Technologies, Hayward, CA, USA). Each data point included at least 60,000 events for analysis of mobilized cells.

Use of Animal Subjects. All experimental protocols were approved and performed in accordance with the guidelines defined by the Institutional Animal Care and Use Committee (IACUC) of National Health Research Institutes (NHRI), Taiwan, R.O.C.

ASSOCIATED CONTENT

Supporting Information

MD of compound **25**:CXCR4 (PDB code 3OE0) complex and the RMSD of the protein backbone of αC atom of amino acids during the MD simulations; the NMR spectra of the key compounds, **18**, **24**, and **25** and the synthesis of compounds **IIa-IIc**, **IVa-IVc**, **Va-Vc**, **18-I**, **18-II**, **18-III**, **19-I**, **19-II** and **19-III**; procedures of CXCR2, CCR2, CCR4, CCR5 radioligand binding assays and CXCR7 beta-arrestin assay are described in supporting information. This material is available free of charge via the Internet at http://pubs.acs.org.

AUTHOR INFORMATION

Corresponding Authors

* Telephone: +886-37-246-166 ext. 35709. Fax: + 886-37-586-456. E-mail: ksshia@nhri.org.tw

* Telephone: +886-37-246-166 ext. 35769. Fax: + 886-37-586-456. E-mail: kelvintsou@nhri.org.tw

Author Contributions

†These authors contributed equally to this work.

Notes

The authors declare no competing financial interest.

ACKNOWLEDGMENTS

We are grateful to the National Health Research Institutes and Ministry of Science and Technology of the Republic of China (MOST 101-2325-B-400-016) and Public Health Service grant AI-38204 from the National Institutes of Health for financial support. Yung-Chi Cheng is a fellow of National Foundation for Cancer Research (USA) and thanks NIH (5R01A1038204-20) for financial support.

ABBREVIATIONS USED

HAART, Highly Active Antiretroviral Therapy; gp120, glycoprotein 120; SDF-1α, stromal-derived factor-1α; SAR, structure−activity relationships; MD, molecular dynamics; mpk, milligram per kilogram; V3 loop, third variable loop.

REFERENCES

1. Montaner, J. S.; Hogg, R.; Wood, E.; Kerr, T.; Tyndall, M.; Levy, A. R.; Harrigan, P. R. The case for expanding access to highly active antiretroviral therapy to curb the growth of the HIV epidemic. *Lancet* **2006,** 368, 531-6.

2. Yeni, P. G.; Hammer, S. M.; Carpenter, C. C.; Cooper, D. A.; Fischl, M. A.; Gatell, J. M.; Gazzard, B. G.; Hirsch, M. S.; Jacobsen, D. M.; Katzenstein, D. A.; Montaner, J. S.; Richman, D. D.; Saag, M. S.; Schechter, M.; Schooley, R. T.; Thompson, M. A.; Vella, S.; Volberding, P. A. Antiretroviral treatment for adult HIV infection in 2002: updated recommendations of the International AIDS Society-USA Panel. *JAMA* **2002,** 288, 222-35.

3. Feng, Y.; Broder, C. C.; Kennedy, P. E.; Berger, E. A. HIV-1 entry cofactor: functional cDNA cloning of a seven-transmembrane, G protein-coupled receptor. *Science* **1996,** 272, 872-7.

4. Deng, H.; Liu, R.; Ellmeier, W.; Choe, S.; Unutmaz, D.; Burkhart, M.; Di Marzio, P.; Marmon, S.; Sutton, R. E.; Hill, C. M.; Davis, C. B.; Peiper, S. C.; Schall, T. J.; Littman, D. R.; Landau, N. R. Identification of a major co-receptor for primary isolates of HIV-1. *Nature* **1996,** 381, 661-6.

5. Trkola, A.; Dragic, T.; Arthos, J.; Binley, J. M.; Olson, W. C.; Allaway, G. P.; Cheng-Mayer, C.; Robinson, J.; Maddon, P. J.; Moore, J. P. CD4-dependent, antibody-sensitive interactions between HIV-1 and its co-receptor CCR-5. *Nature* **1996,** 384, 184-7.

6. Dragic, T.; Litwin, V.; Allaway, G. P.; Martin, S. R.; Huang, Y.; Nagashima, K. A.; Cayanan, C.; Maddon, P. J.; Koup, R. A.; Moore, J. P.; Paxton, W. A. HIV-1 entry into CD4+ cells is mediated by the chemokine receptor CC-CKR-5. *Nature* **1996,** 381, 667-73.

7. Alkhatib, G.; Combadiere, C.; Broder, C. C.; Feng, Y.; Kennedy, P. E.; Murphy, P. M.; Berger, E. A. CC CKR5: a RANTES, MIP-1alpha, MIP-1beta receptor as a fusion cofactor for macrophage-tropic HIV-1. *Science* **1996,** 272, 1955-8.

8. Choe, H.; Farzan, M.; Sun, Y.; Sullivan, N.; Rollins, B.; Ponath, P. D.; Wu, L.; Mackay, C. R.; LaRosa, G.; Newman, W.; Gerard, N.; Gerard, C.; Sodroski, J. The beta-chemokine receptors CCR3 and CCR5 facilitate infection by primary HIV-1 isolates. *Cell* **1996,** 85, 1135-48.

9. Wilen, C. B.; Tilton, J. C.; Doms, R. W. Molecular mechanisms of HIV entry. *Adv Exp Med Biol* **2012,** 726, 223-42.

10. Williams, I. G. Enfuvirtide (Fuzeon): the first fusion inhibitor. *Int J Clin Pract* **2003,** 57, 890-7.

11. Fletcher, C. V. Enfuvirtide, a new drug for HIV infection. *Lancet* **2003,** 361, 1577-8.

12. Gulick, R. M.; Lalezari, J.; Goodrich, J.; Clumeck, N.; DeJesus, E.; Horban, A.; Nadler, J.; Clotet, B.; Karlsson, A.; Wohlfeiler, M.; Montana, J. B.; McHale, M.; Sullivan, J.; Ridgway, C.; Felstead, S.; Dunne, M. W.; van der Ryst, E.; Mayer, H.; Teams, M. S. Maraviroc for previously treated patients with R5 HIV-1 infection. *N Engl J Med* **2008,** 359, 1429-41.

13. Westby, M.; Lewis, M.; Whitcomb, J.; Youle, M.; Pozniak, A. L.; James, I. T.; Jenkins, T. M.; Perros, M.; van der Ryst, E. Emergence of CXCR4-using human immunodeficiency virus type 1 (HIV-1) variants in a minority of HIV-1-infected patients following treatment with the CCR5 antagonist maraviroc is from a pretreatment CXCR4-using virus reservoir. *J Virol* **2006,** 80, 4909-20.

14. Muller, A.; Homey, B.; Soto, H.; Ge, N.; Catron, D.; Buchanan, M. E.; McClanahan, T.; Murphy, E.; Yuan, W.; Wagner, S. N.; Barrera, J. L.; Mohar, A.; Verastegui, E.; Zlotnik, A. Involvement of chemokine receptors in breast cancer metastasis. *Nature* **2001,** 410, 50-6.

15. Balkwill, F. Cancer and the chemokine network. *Nat Rev Cancer* **2004,** 4, 540-50.

16. Balkwill, F. The significance of cancer cell expression of the chemokine receptor CXCR4. *Semin Cancer Biol* **2004,** 14, 171-9.

17. Arnolds, K. L.; Spencer, J. V. CXCR4: a virus's best friend? *Infect Genet Evol* **2014,** 25, 146-56.

18. Tamamis, P.; Floudas, C. A. Elucidating a key component of cancer metastasis: CXCL12 (SDF-1alpha) binding to CXCR4. *J Chem Inf Model* **2014,** 54, 1174-88.

19. Connor, R. I.; Sheridan, K. E.; Ceradini, D.; Choe, S.; Landau, N. R. Change in coreceptor use correlates with disease progression in HIV-1--infected individuals. *J Exp Med* **1997,** 185, 621-8.

20. Raymond, S.; Delobel, P.; Mavigner, M.; Cazabat, M.; Encinas, S.; Souyris, C.; Bruel, P.; Sandres-Saune, K.; Marchou, B.; Massip, P.; Izopet, J. CXCR4-using viruses in plasma and peripheral

blood mononuclear cells during primary HIV-1 infection and impact on disease progression. *AIDS* **2010,** 24, 2305-12.

21. Sucupira, M. C.; Sanabani, S.; Cortes, R. M.; Giret, M. T.; Tomiyama, H.; Sauer, M. M.; Sabino, E. C.; Janini, L. M.; Kallas, E. G.; Diaz, R. S. Faster HIV-1 disease progression among Brazilian individuals recently infected with CXCR4-utilizing strains. *PLoS One* **2012,** 7, e30292.

22. Schuitemaker, H.; Koot, M.; Kootstra, N. A.; Dercksen, M. W.; de Goede, R. E.; van Steenwijk, R. P.; Lange, J. M.; Schattenkerk, J. K.; Miedema, F.; Tersmette, M. Biological phenotype of human immunodeficiency virus type 1 clones at different stages of infection: progression of disease is associated with a shift from monocytotropic to T-cell-tropic virus population. *J Virol* **1992,** 66, 1354-60.

23. Grande, F.; Garofalo, A.; Neamati, N. Small molecules anti-HIV therapeutics targeting CXCR4. *Curr Pharm Des* **2008,** 14, 385-404.

24. Bleul, C. C.; Farzan, M.; Choe, H.; Parolin, C.; Clark-Lewis, I.; Sodroski, J.; Springer, T. A. The lymphocyte chemoattractant SDF-1 is a ligand for LESTR/fusin and blocks HIV-1 entry. *Nature* **1996,** 382, 829-33.

25. Arenzana-Seisdedos, F.; Virelizier, J. L.; Rousset, D.; Clark-Lewis, I.; Loetscher, P.; Moser, B.; Baggiolini, M. HIV blocked by chemokine antagonist. *Nature* **1996,** 383, 400.

26. Signoret, N.; Oldridge, J.; Pelchen-Matthews, A.; Klasse, P. J.; Tran, T.; Brass, L. F.; Rosenkilde, M. M.; Schwartz, T. W.; Holmes, W.; Dallas, W.; Luther, M. A.; Wells, T. N.; Hoxie, J. A.; Marsh, M. Phorbol esters and SDF-1 induce rapid endocytosis and down modulation of the chemokine receptor CXCR4. *J Cell Biol* **1997,** 139, 651-64.

27. Donzella, G. A.; Schols, D.; Lin, S. W.; Este, J. A.; Nagashima, K. A.; Maddon, P. J.; Allaway, G. P.; Sakmar, T. P.; Henson, G.; De Clercq, E.; Moore, J. P. AMD3100, a small molecule inhibitor of HIV-1 entry via the CXCR4 co-receptor. *Nat Med* **1998,** 4, 72-7.

28. Skerlj, R. T.; Bridger, G. J.; Kaller, A.; McEachern, E. J.; Crawford, J. B.; Zhou, Y.; Atsma, B.; Langille, J.; Nan, S.; Veale, D.; Wilson, T.; Harwig, C.; Hatse, S.; Princen, K.; De Clercq, E.; Schols, D. Discovery of novel small molecule orally bioavailable C-X-C chemokine receptor 4

antagonists that are potent inhibitors of T-tropic (X4) HIV-1 replication. *J Med Chem* **2010,** 53, 3376-88.

29. Wu, B.; Chien, E. Y.; Mol, C. D.; Fenalti, G.; Liu, W.; Katritch, V.; Abagyan, R.; Brooun, A.; Wells, P.; Bi, F. C.; Hamel, D. J.; Kuhn, P.; Handel, T. M.; Cherezov, V.; Stevens, R. C. Structures of the CXCR4 chemokine GPCR with small-molecule and cyclic peptide antagonists. *Science* **2010,** 330, 1066-71.

30. Tamamis, P.; Floudas, C. A. Molecular recognition of CXCR4 by a dual tropic HIV-1 gp120 V3 loop. *Biophys J* **2013,** 105, 1502-14.

31. Debnath, B.; Xu, S.; Grande, F.; Garofalo, A.; Neamati, N. Small molecule inhibitors of CXCR4. *Theranostics* **2013,** 3, 47-75.

32. Choi, W. T.; Duggineni, S.; Xu, Y.; Huang, Z.; An, J. Drug discovery research targeting the CXC chemokine receptor 4 (CXCR4). *J Med Chem* **2012,** 55, 977-94.

33. Wu, C. H.; Chang, C. P.; Song, J. S.; Jan, J. J.; Chou, M. C.; Wu, S. H.; Yeh, K. C.; Wong, Y. C.; Hsieh, C. J.; Chen, C. T.; Kao, T. T.; Wu, S. Y.; Yeh, C. F.; Tseng, C. T.; Chao, Y. S.; Shia, K. S. Discovery of novel stem cell mobilizers that target the CXCR4 receptor. *ChemMedChem* **2012,** 7, 209-12.

34. Choi, W. T.; Kumar, S.; Madani, N.; Han, X.; Tian, S.; Dong, C. Z.; Liu, D.; Duggineni, S.; Yuan, J.; Sodroski, J. G.; Huang, Z.; An, J. A novel synthetic bivalent ligand to probe chemokine receptor CXCR4 dimerization and inhibit HIV-1 entry. *Biochemistry* **2012,** 51, 7078-86.

35. Tian, S.; Choi, W. T.; Liu, D.; Pesavento, J.; Wang, Y.; An, J.; Sodroski, J. G.; Huang, Z. Distinct functional sites for human immunodeficiency virus type 1 and stromal cell-derived factor 1alpha on CXCR4 transmembrane helical domains. *J Virol* **2005,** 79, 12667-73.

36. Brelot, A.; Heveker, N.; Montes, M.; Alizon, M. Identification of residues of CXCR4 critical for human immunodeficiency virus coreceptor and chemokine receptor activities. *J Biol Chem* **2000,** 275, 23736-44.

37. Choi, W. T.; Tian, S.; Dong, C. Z.; Kumar, S.; Liu, D.; Madani, N.; An, J.; Sodroski, J. G.; Huang, Z. Unique ligand binding sites on CXCR4 probed by a chemical biology approach:

implications for the design of selective human immunodeficiency virus type 1 inhibitors. *J Virol* **2005,** 79, 15398-404.

38. Chabot, D. J.; Zhang, P. F.; Quinnan, G. V.; Broder, C. C. Mutagenesis of CXCR4 identifies important domains for human immunodeficiency virus type 1 X4 isolate envelope-mediated membrane fusion and virus entry and reveals cryptic coreceptor activity for R5 isolates. *J Virol* **1999,** 73, 6598-609.

39. Zhou, N.; Luo, Z.; Luo, J.; Liu, D.; Hall, J. W.; Pomerantz, R. J.; Huang, Z. Structural and functional characterization of human CXCR4 as a chemokine receptor and HIV-1 co-receptor by mutagenesis and molecular modeling studies. *J Biol Chem* **2001,** 276, 42826-33.

40. Brelot, A.; Heveker, N.; Adema, K.; Hosie, M. J.; Willett, B.; Alizon, M. Effect of mutations in the second extracellular loop of CXCR4 on its utilization by human and feline immunodeficiency viruses. *J Virol* **1999,** 73, 2576-86.

41. Burns, J. M.; Summers, B. C.; Wang, Y.; Melikian, A.; Berahovich, R.; Miao, Z.; Penfold, M. E.; Sunshine, M. J.; Littman, D. R.; Kuo, C. J.; Wei, K.; McMaster, B. E.; Wright, K.; Howard, M. C.; Schall, T. J. A novel chemokine receptor for SDF-1 and I-TAC involved in cell survival, cell adhesion, and tumor development. *J Exp Med* **2006,** 203, 2201-13.

42. Zabel, B. A.; Wang, Y.; Lewen, S.; Berahovich, R. D.; Penfold, M. E.; Zhang, P.; Powers, J.; Summers, B. C.; Miao, Z.; Zhao, B.; Jalili, A.; Janowska-Wieczorek, A.; Jaen, J. C.; Schall, T. J. Elucidation of CXCR7-mediated signaling events and inhibition of CXCR4-mediated tumor cell transendothelial migration by CXCR7 ligands. *J Immunol* **2009,** 183, 3204-11.

43. Crump, M. P.; Gong, J. H.; Loetscher, P.; Rajarathnam, K.; Amara, A.; Arenzana-Seisdedos, F.; Virelizier, J. L.; Baggiolini, M.; Sykes, B. D.; Clark-Lewis, I. Solution structure and basis for functional activity of stromal cell-derived factor-1; dissociation of CXCR4 activation from binding and inhibition of HIV-1. *EMBO J* **1997,** 16, 6996-7007.

44. Paintsil, E.; Dutschman, G. E.; Hu, R.; Grill, S. P.; Lam, W.; Baba, M.; Tanaka, H.; Cheng, Y. C. Intracellular metabolism and persistence of the anti-human immunodeficiency virus activity of

2',3'-didehydro-3'-deoxy-4'-ethynylthymidine, a novel thymidine analog. *Antimicrob Agents Chemother* **2007,** 51, 3870-9.

45. Brooks, B. R.; Brooks, C. L., 3rd; Mackerell, A. D., Jr.; Nilsson, L.; Petrella, R. J.; Roux, B.; Won, Y.; Archontis, G.; Bartels, C.; Boresch, S.; Caflisch, A.; Caves, L.; Cui, Q.; Dinner, A. R.; Feig, M.; Fischer, S.; Gao, J.; Hodoscek, M.; Im, W.; Kuczera, K.; Lazaridis, T.; Ma, J.; Ovchinnikov, V.; Paci, E.; Pastor, R. W.; Post, C. B.; Pu, J. Z.; Schaefer, M.; Tidor, B.; Venable, R. M.; Woodcock, H. L.; Wu, X.; Yang, W.; York, D. M.; Karplus, M. CHARMM: the biomolecular simulation program. *J Comput Chem* **2009,** 30, 1545-614.

46. Berendsen, H. J. C.; van der Spoel, D.; van Drunen, R. GROMACS: A message-passing parallel molecular dynamics implementation. *Computer Physics Communications* **1995,** 91, 43-56.

47. Hess, B.; Kutzner, C.; van der Spoel, D.; Lindahl, E. GROMACS 4: Algorithms for Highly Efficient, Load-Balanced, and Scalable Molecular Simulation. *Journal of Chemical Theory and Computation* **2008,** 4, 435-447.

48. Schuttelkopf, A. W.; van Aalten, D. M. PRODRG: a tool for high-throughput crystallography of protein-ligand complexes. *Acta Crystallogr D Biol Crystallogr* **2004,** 60, 1355-63.

49. Chiu, S. W.; Pandit, S. A.; Scott, H. L.; Jakobsson, E. An improved united atom force field for simulation of mixed lipid bilayers. *J Phys Chem B* **2009,** 113, 2748-63.

50. B. Hess, H. B., H. J. C. Berendsen and J. G. E. M. Fraaije. *J. Comp. Chem* **1997,** 18, 1463-1472.

Scheme 1. **Synthetic Procedures for Quinazoline Compounds 9-11**[a]

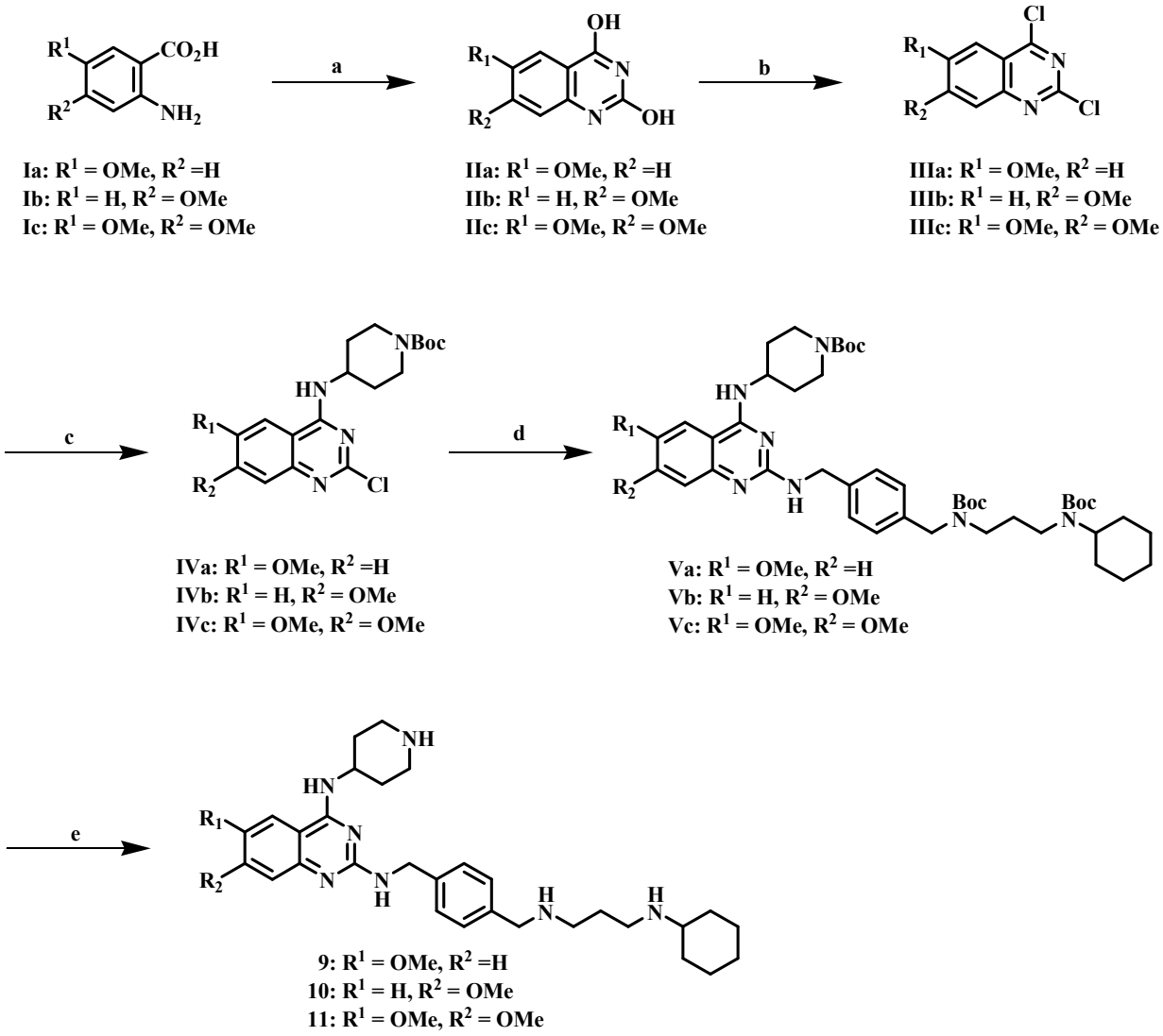

[a]Reagents and conditions: (a) urea, 200 ^{o}C, 2 h, 80-85%; (b) $POCl_3$, 2-ethyl-pyridine, 110 ^{o}C, 3h; (c) 4-amino-1-Boc-piperidine, Et_3N, DCM, -5 ^{o}C to RT, 16 h, 54-59% over two steps; (d) side chain D, 1-pentanol, microwave, 120 ^{o}C, 15 min, 59-63%; (e) 1N HCl in diethylether, DCM, 16 h, 83-92%.

Scheme 2. **Synthetic Procedures for Compound 18**[a]

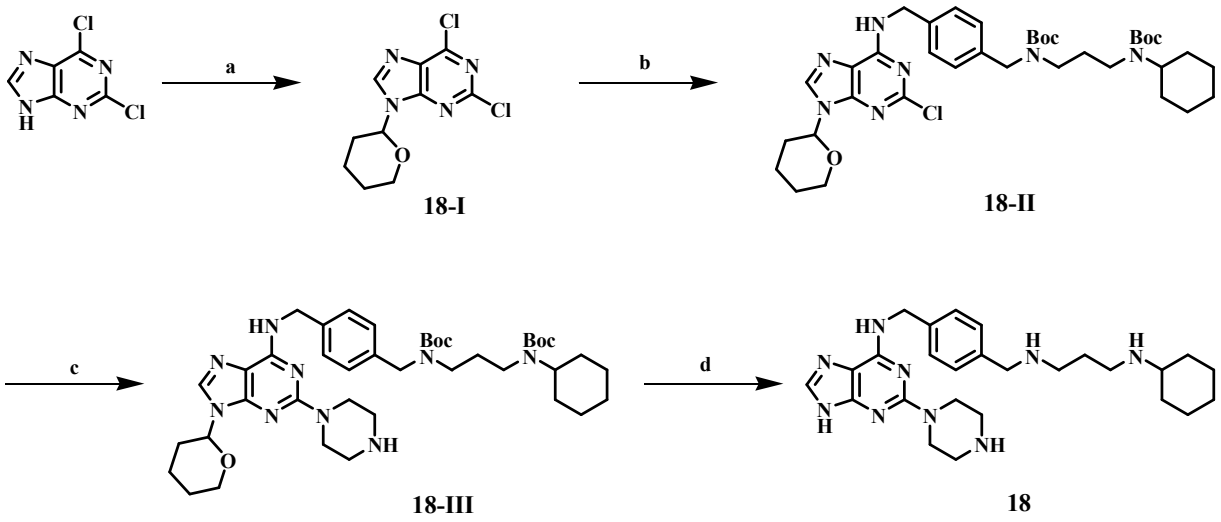

[a]Reagents and conditions: (a) 3,4-dihydro-2*H*-pyran, 25 ^{o}C, 15 h, 100%; (b) side chain D, TEA, DCM, 50 ^{o}C, 4 h, 62%; (c) piperazine, 1-pentanol, 100 ^{o}C, 15 h, 64%; (d) 1N HCl in diethylether, DCM, 16 h, 94%.

Scheme 3. A **Synthetic Procedure for Compound 19**[a]

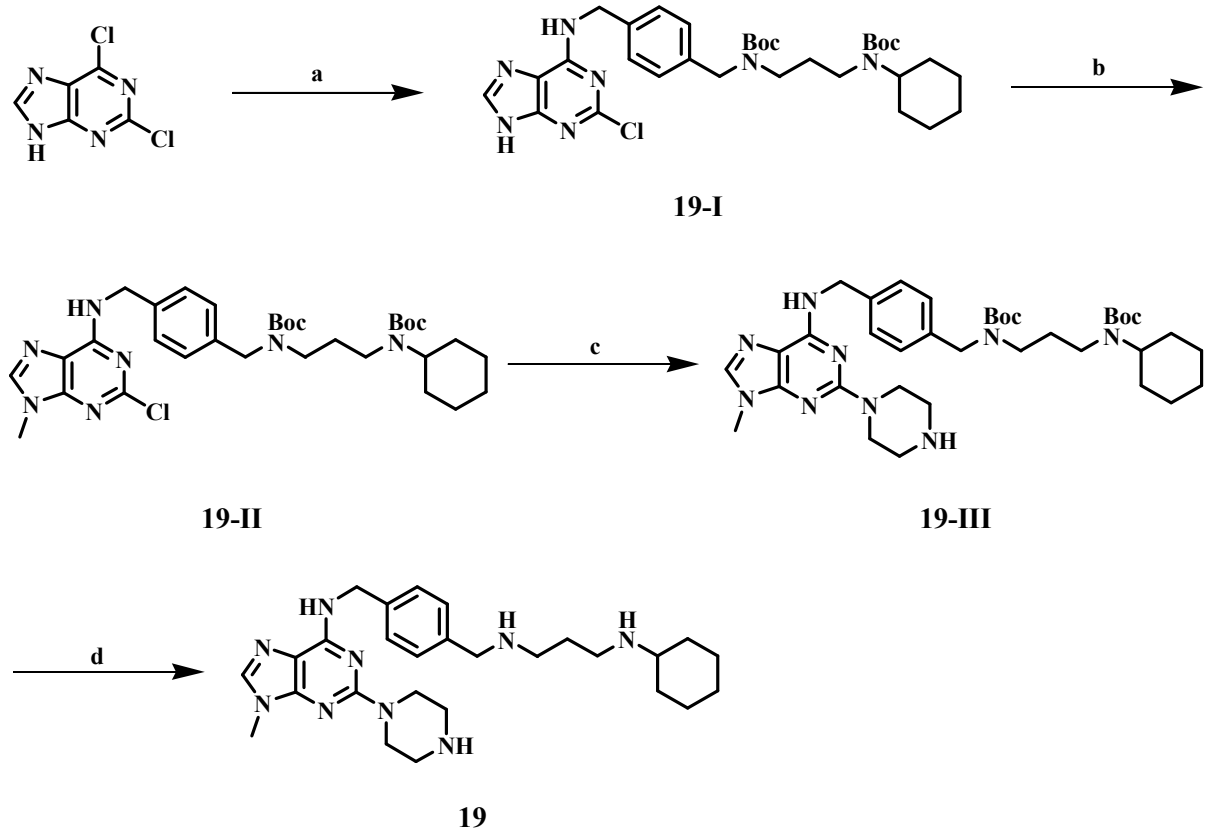

[a]Reagents and conditions: (a) side chain D, TEA, *t*-BuOH, 50 ^{o}C, 4 h, 89%; (b) MeI, K_2CO_3, DMF, 25 ^{o}C, 3 h, 97%; (c) piperazine, ethylene glycol monomethyl ether, 120 ^{o}C, 15 h, 69%; (d) 1N HCl in diethylether, DCM, 16 h, 91%.

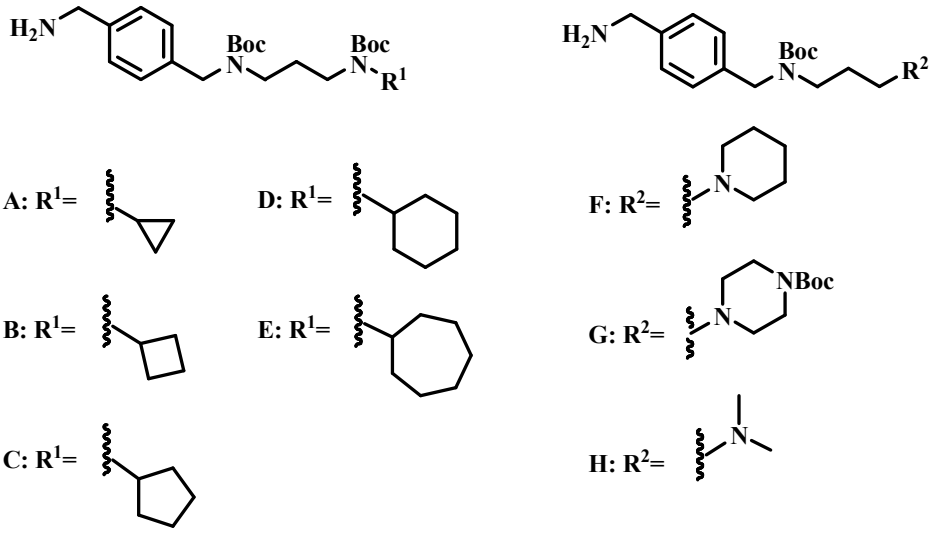

Figure 1. Side chains **A-H**.

Table 1. Biological Evaluation of Quinazoline Core Polyamines Derivatives on CXCR4-binding and HIV Inhibitory Profiles

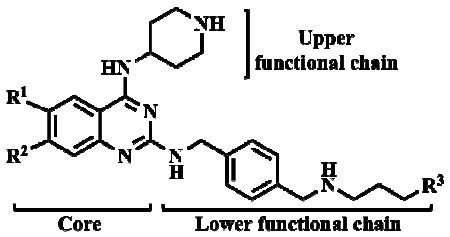

Compound 1-17

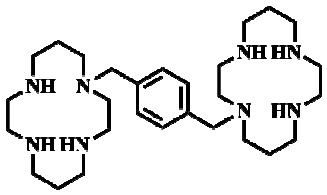

AMD3100

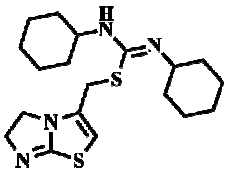

IT1t

Compound	R^1	R^2	R^3	CXCR4 IC_{50} (nM)[a]	Anti-HIV EC_{50} (nM)	Cytotoxicity CC_{50} (μM) CEM	Cytotoxicity CC_{50} (μM) TZM-bl	Selective Index CC_{50} / EC_{50} CEM	Selective Index CC_{50} / EC_{50} TZM-bl
1	H	H		877.5 ± 7.8	161.2 ± 22.9	2 ± 0.8	ND	12	ND
2	H	H		50.0 ± 14.3	111.1 ± 11.2	5.2 ± 1.3	4.3 ± 0.3	47	39
3	H	H		83.5 ± 10.8	48.9 ± 8.0	22.6 ± 1.2	16.9 ± 1.9	462	346
4	H	H		36.2 ± 1.4	68.4 ± 8.0	> 50	> 50	>731	>731
5	H	H		44.8 ± 1.4	58.7 ± 7.6	23 ± 4.8	42.2 ± 3.7	392	719
6	H	H		35.2 ± 3.0	71.5 ± 29.0	3.2 ± 0.8	3.4 ± 0.1	45	48
7	H	H		3149.0 ± 362.0	>500	37.5 ± 7.0	24.6 ± 0.5	ND	ND
8	H	H		>10000	>500	32.2 ± 3.0	24.2 ± 0.6	ND	ND
9	OMe	H		8.7 ± 1.1	47.4 ± 18.3	8 ± 1.7	8.4 ± 1.0	169	177
10	H	OMe		6.8 ± 1.8	8.6 ± 5.3	1.6 ± 0.6	10.8 ± 3.3	186	1256
11	OMe	OMe		31.5 ± 3.0	21.7 ± 3.0	17.5 ± 2.4	23.1 ± 7.0	806	1065
12	OMe	H		7.9 ± 0.6	42.6 ± 7.0	6.5 ± 1.1	21.7 ± 7.0	153	509
13	H	OMe		12.8 ± 4.3	45.4 ± 8.4	6.1 ± 1.1	10.8 ± 0.8	134	238
14	OMe	OMe		78.4 ± 19.2	48.4 ± 3.4	18.2 ± 4.5	19.3 ± 0.88	376	399
15	OMe	H		66.0 ± 28.3	93.9 ± 14.7	18.4 ± 5.5	24.5 ± 2.5	196	261
16	H	OMe		47.9 ± 23.1	27.0 ± 4.2	13.8 ± 1.9	32.2 ± 0.2	511	1193
17	OMe	OMe		87.8 ± 15.0	26.2 ± 4.4	17.6 ± 3.0	28.1 ± 1.5	672	1073
AMD3100	-	-	-	213.1 ± 26.2	66.6 ± 23.1	-	-	-	-
IT1t	-	-	-	100.6 ± 23.1	> 70	-	-	-	-

[a]Determined by 50% inhibition of radioligand [125I]SDF-1α binding to hCXCR4-transfected HEK293 membrane; values represent the mean ± SD of at least three independent experiments.

Table 2. Biological Evaluation of Purine core Polyamines Derivatives on CXCR4 and HIV Profiles

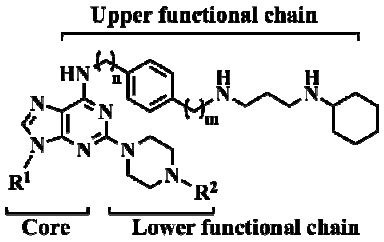

18-20, 23, 24

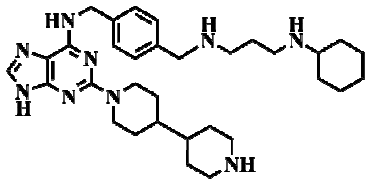

21

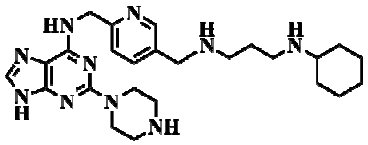

22

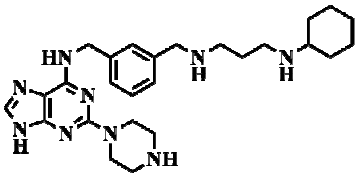

25

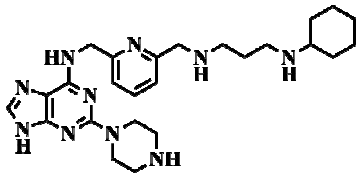

26

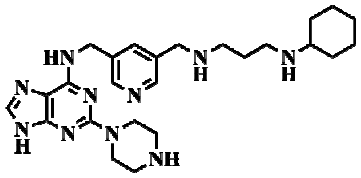

27

Compound	R^1	R^2	n, m	CXCR4 IC_{50} (nM)[a]	Anti-HIV EC_{50} (nM)	Cytotoxicity CC_{50} (μM)		Selective Index CC_{50} / EC_{50}	
						CEM	TZM-bl	CEM	TZM-bl
18	H	H	1, 1	18.1 ± 2.8	2.0 ± 0.1	> 50	> 50	>25,000	>25000
19	Me	H	1, 1	86.2 ± 28.8	3.4 ± 0.2	20.2 ± 1.5	18.6 ± 2	5,941	5,470
20	Me	Me	1, 1	59.5 ± 11.9	6.5 ± 0.2	13.8 ± 1.8	11.2 ± 2.1	2,123	1,723
21	-	-	-	51.6 ± 11.8	84.3 ± 15.8	>50	>50	>593	>593
22	-	-	-	45.9±0.1	4.2 ± 0.3	> 50	> 50	>11,905	>11,905
23	H	H	2, 1	45.1 ± 3.7	3.1 ± 0.7	46.7 ± 3.2	> 50	15,065	>16,129
24	H	H	1, 2	16.4 ± 3.5	0.51 ± 0.02	> 50	> 50	>98,039	>98,039
25	-	-	-	4.2 ± 0.4	0.61 ± 0.27	>50	>50	>83,333	>83,333
26	-	-	-	32.9 ± 2.3	2.5 ± 0.1	>50	>50	>20,000	>20,000
27	-	-	-	44.1±17.3	5.7 ± 1.0	>50	>50	>8,772	>8,772

[a]Determined by 50% inhibition of radioligand $[^{125I}]$SDF-1 binding to hCXCR4-transfected HEK293 membrane; values represent the mean ± SD of at least three independent experiments.

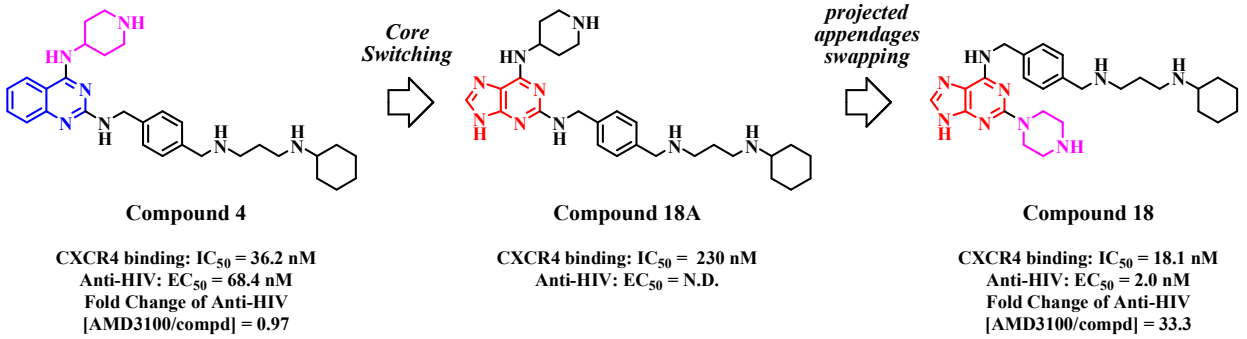

Compound 4

CXCR4 binding: IC_{50} = 36.2 nM
Anti-HIV: EC_{50} = 68.4 nM
Fold Change of Anti-HIV
[AMD3100/compd] = 0.97

Compound 18A

CXCR4 binding: IC_{50} = 230 nM
Anti-HIV: EC_{50} = N.D.

Compound 18

CXCR4 binding: IC_{50} = 18.1 nM
Anti-HIV: EC_{50} = 2.0 nM
Fold Change of Anti-HIV
[AMD3100/compd] = 33.3

Figure 2. IC_{50} of compounds **4, 18, 18A.** The enhancement of Anti-HIV activity is illustrated by the fold change between the anti-HIV activities of AMD3100 to those of compounds **4** and **18**.

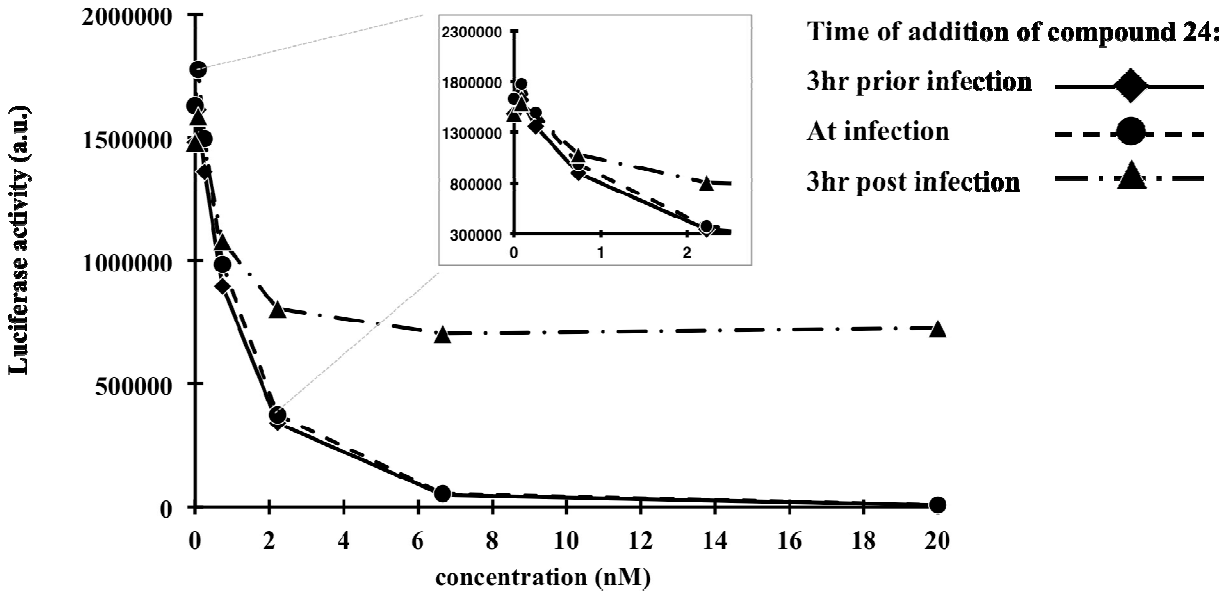

Figure 3. Cell-based time-of-addition assay over one HIV replication cycle. Compound **24**, at different concentrations, was added three hours before, simultaneously with, and three hours after HIV-1 infection. Inset is a magnified view of indicated portion of the main chart.

Table 3. Specificity of Compounds 24 and 25 against Related Chemokine Receptors

Compound	Parameter	CXCR4	CXCR2	CCR2	CCR4	CCR5
24	Inhibition (%)[a]	100	16	10	11	15
	IC_{50} (nM)	16.4	>10,000	>10,000	>10,000	>10,000
	Selective Index	-	>609	>609	>609	>609
25	Inhibition (%)[a]	100	12	2	0	14
	IC_{50} (nM)	4.2	>10,000	>10,000	>10,000	>10,000
	Selective Index	-	>2,380	>2,380	>2,380	>2,380

[a] Percent inhibition was determined at 10 μM; weak inhibition was observed for all tested chemokine receptors except CXCR4.

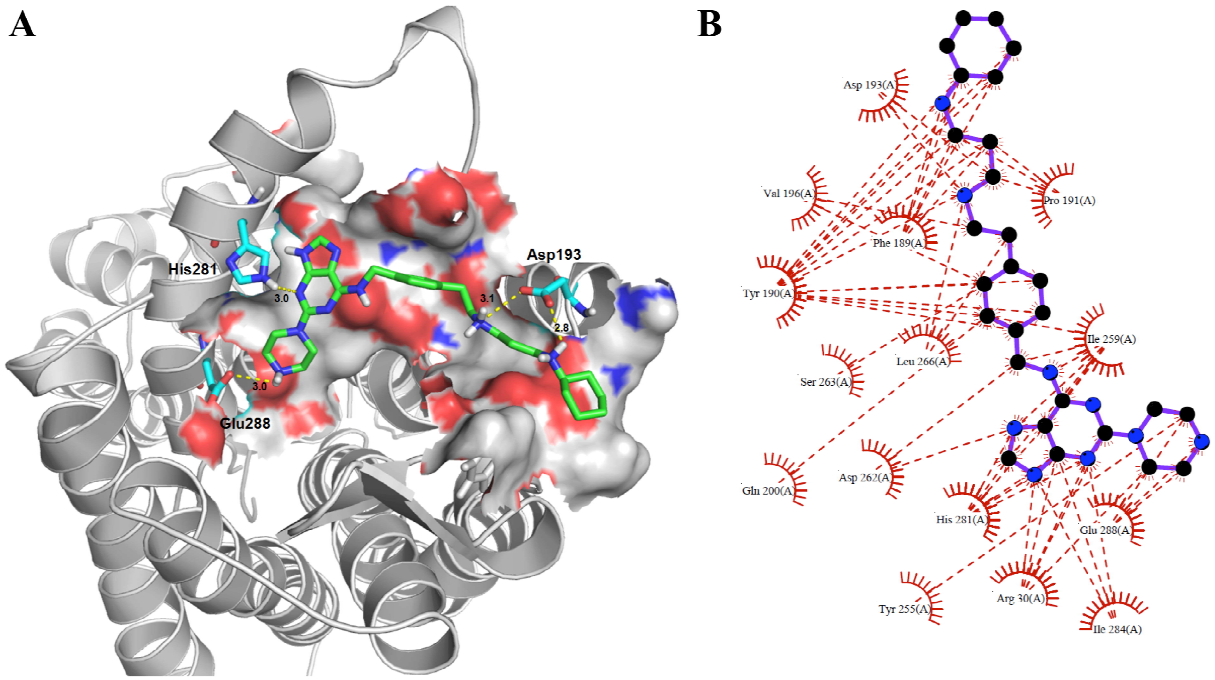

Figure 4. Molecular dynamics simulations between compound **24** and CXCR4 (PDB code 3OE0) receptor. **A**. Structure of CXCR4-**24** complex after 20 ns of molecular dynamics (MD) simulations. The hydrogen bonding network (yellow lines) reveals strong hydrogen bondings around compound **24** (green) with the residues of Asp193, His281, and Glu288 (cyan). **B**. Ligplot diagram showing hydrophobic interactions between the indicated CXCR4 amino acid residues and compound **24** after 20 ns of MD simulation.

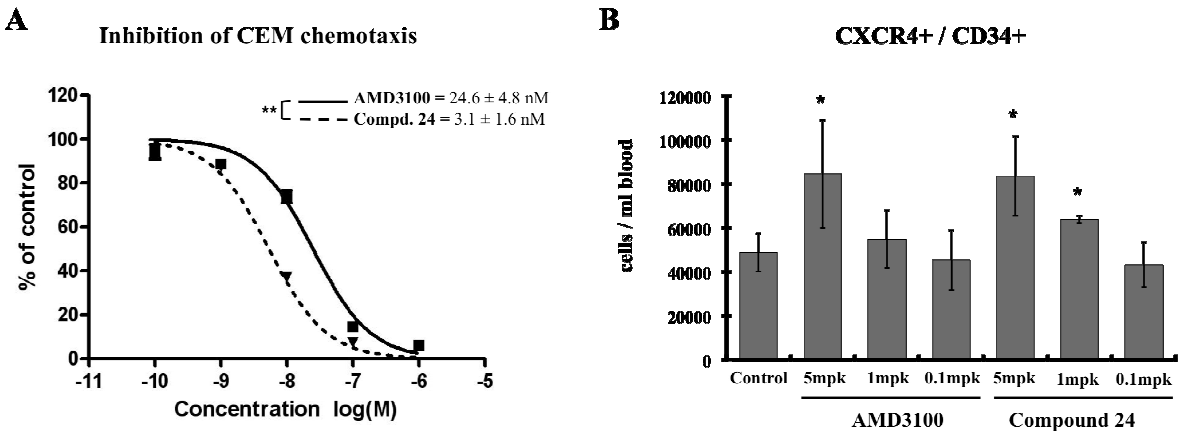

Figure 5. Functional studies by compound **24**. **A.** SDF-1α-induced chemotaxis assay. Inhibition of CEM cell chemotaxis at various concentrations of compound **24** and AMD3100. **B**. C57BL/6 mice were subcutaneously administered with the vehicle control, AMD3100, or compound **24** at different doses, respectively; 2 hours after dosing, the peripheral blood was harvested for analyzing the cell type of interest.

Table of Contents Graphic